CHALMERS
UNIVERSITY OF TECHNOLOGY

Accuracy Evaluation of Power System State Estimation

An evaluative study of the accuracy of state estimation with application to parameter estimation

Master of Science Thesis in Electric Power Engineering

HANNES HAGMAR

Department of Energy and Environment
Division of Electric Power Engineering
CHALMERS UNIVERSITY OF TECHNOLOGY
Gothenburg, Sweden, 2016

Master of Science Thesis 2016:04

Accuracy Evaluation of Power System State Estimation

An evaluative study of the accuracy of state estimation with application to parameter estimation

HANNES HAGMAR

Department of Energy and Environment
Division of Electric Power Engineering
CHALMERS UNIVERSITY OF TECHNOLOGY
Gothenburg, Sweden, 2016

Accuracy evaluation of Power System State Estimation - an evaluative study of the accuracy of state estimation with application to parameter estimation

HANNES HAGMAR

Department of Energy and Environment

Division of Electric Power Engineering

Chalmers University of Technology

SE-412 96 Gothenburg

Sweden

Telephone +46(0)31-772 1000

Thesis supervisor
Anders Lindskog, Scientist
SP Technical Research Institute of Sweden
Telephone +46705-885841
Email anders.lindskog@sp.se

Thesis examiner
Anh Tuan Le, Senior Lecturer
Department of Energy and Environment
Division of Electric Power Engineering
Chalmers University of Technology, Gothenburg, Sweden
Telephone +46(0)31-772 1000
E-mail tuan.le@chalmers.se

Printed by Chalmers Reproservice

Gothenburg, Sweden 2016

Accuracy evaluation of Power System State Estimation - an evaluative study of the accuracy of state estimation with application to parameter estimation

HANNES HAGMAR
Department of Energy and Environment
Division of Electric Power Engineering
Chalmers University of Technology

Abstract

The following report examines the impact that parameter and model errors have on the result of the power system state estimation. Furthermore, the feasibility of increasing the accuracy of the state estimation is examined by introducing parameter estimation within the ordinary estimation model.

Model errors due to unbalanced grid conditions are found to have a large impact on the phase values, but an almost negligible impact on the averaged values that are commonly used as input to the state estimation model. Parameter errors affect the accuracy of the state estimation in various extents, and errors in the line susceptance are found to generally cause the largest errors. The level of measurement redundancy is significant to the result, and reduced measurement redundancy will in general increase the estimation errors due to parameter errors. Furthermore, undesirable combinations of parameter errors within a larger network are also found to increase the estimation errors significantly. In order to estimate the magnitude of estimation errors caused by parameter errors, each grid configuration and power flow state would have to be examined individually.

Parameter estimation was found to be highly accurate in estimating the line susceptance for most levels of reasonable measurement errors. However, the line conductance and shunt susceptance were found to be significantly harder to estimate and even small measurement errors resulted in poor estimations. Using parameter estimation for the line susceptance under conditions of relatively low levels of measurement errors was found to significantly decrease the errors in the state estimation. Finally, an alternative method of estimating the line conductance was examined. This estimation was found to be more resilient to errors in the voltage measurement, but was still sensitive to errors in the power flow measurement devices.

Keywords: *State estimation, parameter estimation, sensitivity analysis, parameter errors, model errors, SP, Svenska kraftnät, accuracy evaluation, state estimation accuracy enhancement*

Preface

The following report is a part of a Master of Science thesis within the electrical power engineering program at Chalmers University in Gothenburg, Sweden. The project has been conducted in cooperation with SP Technical Research Institute of Sweden on behalf of the Swedish national power grid operator Svenska kraftnät. To ease the comprehension of the tables and figures it is recommended that the report is reprinted in colour. The author of the report is the creator of all figures unless specifically stated otherwise.

This report is a result of many hours of work and significant amounts of hot, black coffee. Initially, I would like to express my gratitude towards Anders Lindskog for his supervision, our discussions, and the inputs during this time. I would also like to thank Peiyuan Chen for recommending me to SP in the first place, and Anh Tuan Le for being my examiner.

Then of course, my highest gratitude is towards Lina who has, despite perhaps not the best knowledge in electric power, thoroughly proofread my report and been the best support imaginable.

Hannes Hagmar, 2nd of May 2016

Contents

Appendices

Abbreviations

LNRT	Largest Normalized Residual Test
MLE	Maximum Likelihood Estimation
PE	Parameter Estimation
SCADA	Supervisory Control and Data Acquisition
SE	State Estimation
SP	SP Technical Research Institute of Sweden
Svk	Svenska kraftnät (TSO of SWEDEN)
SWEDAC	Swedish Board for Accreditation and Conformity Assessment
TSE	Theil-Sen Estimator
WLS	Weighted Least Squares

List of symbols

σ	Standard deviation
μ	Expected value or mean value
θ_{ij}	Phase angle difference between buses i and j
Ω	Covariance of measurement residual
Λ_{pp}	Block in the inverse of the gain matrix, G
A	Transformation matrix
a	Complex number with the value of $e^{\frac{+j2\pi}{3}}$
e_p	Parameter error
$G(x)$	Gain matrix
G_{ij} and B_{ij}	ijth element of the bus admittance matrix
g_{ij} and b_{ij}	Conductance and susceptance of the series branch connecting the buses i and j
g_{si} and b_{si}	Conductance and susceptance of the shunt branch connected at bus i
H	Jacobian of state vector function
$h(x)$	Nonlinear function that relates state vector to measurement
$h_i(x, p)$	Nonlinear function that relates system states and parameter to the i-th measurement
I_{MAT}	Identity matrix
I_s, I_r, I_L	Sending, receiving, and line current
I_0, I_1, I_2	Zero, positive, and negative sequence current
J	Objective function
K	K-matrix
$P_f, P_{f\%}$	Absolute and relative line losses
$\mathrm{P_i}, \mathrm{Q_i}$	Total active and reactive power injection at bus i
P_{ij}, Q_{ij}	Active and reactive power flow from bus i and j
$p,\ p_o$	Parameter and initial parameter value

R	Covariance matrix (and for some instances line resistance)
r	Residual of measurement
r_i^N	Normalized residual vector
$V_s,\ V_r$	Sending and receiving end voltage
V_0, V_1, V_2	Zero, positive, and negative sequence voltage
$Ve^{j(\omega t+\varphi+x)}$	Phase voltage in vector form
W	Weighting matrix
W_p	Weighting factor assigned to the initial parameter value
Z_d	Off-diagonal elements in the impedance matrix
Z_M	Line impedance matrix
Z_{XX}, Z_{XY}	Mutual and self-impedances
Z_s	Diagonal elements in the impedance matrix
z	Measurement
$\Delta z, \Delta\hat{z}$	Actual and estimated change in linearized measurement equation
Y_M	Line admittance matrix
Y_{XX}, Y_{XY}	Mutual and self-admittances

1 Introduction

The following report is conducted in cooperation with SP Technical Research Institute of Sweden (SP) on behalf of the Swedish transmission system operator Svenska kraftnät (Svk). The report is a part of a master thesis performed within the electrical power engineering program at Chalmers University of Technology in Gothenburg, Sweden.

In March 2014, a research collaboration was initiated between SP and Svk with the main goal of examining the possibilities to continuously supervise the measurement infrastructure through mathematical analysis of real time data from the energy measurement systems in the transmission grid. The following thesis is a part of that research collaboration, and aims to determine the impact that parameter and model errors have on the result of the power system state estimation. Furthermore, the report strives to develop and evaluate methods of parameter estimation.

1.1 Background

The main objective of the power system operation is to maintain the system within the normal secure state while the operating condition varies during the regular operation. This is achieved by monitoring the present state of the system by acquiring measurements from the system and then processing them accordingly. In general, SCADA (Supervisory Control and Data Acquisition) systems are used in order to supervise and gather measurements from the grid, which then allows the system operators to monitor the continuous operation [1].

The state estimation (SE) algorithm is thereafter used to provide the best estimation of the actual state within the power system. The method estimates the system states by using an over-determined system with imperfect measurements. By minimizing the sum of the squares of the differences between the estimated and the measured values of the system, a best estimate of the system is generated. An accurate SE is vital and the result is the backbone of the grid planning and the power system operation. Large errors in the estimation may cause severe flaws in areas such as economic dispatch of power, transient and voltage stability, and the protection system of the grid.

The accuracy of the SE with respect to grid operation is today in general well within the limits to ensure a safe and secure operation. However, an alternative application that the SE tool may be used for is for analysing and detecting errors within the measurement infrastructure. SP has at present the responsibility to inspect and ensure that the energy measurement systems within the transmission grid satisfy the regulated accuracy requirements. These energy measurements are primarily used to register transferred energy, but they may also provide highly accurate instantaneous values of voltages and power that may be used within the SE model. By using the result of the SE and inspecting branches with high residuals, it would be possible to develop methods to identify and correct the errors for these measurements. The same method of detecting measurement errors could then also be applied to the operational measurements that are used by Svk to supervise the grid operation. This method could thus significantly facilitate the fault detection and calibration of measurement devices in the grid.

The general procedure of the SE is to assume that the line model and the line parameters are perfectly known and that it is the measurements that are contaminated with errors and noise. However, this is generally not an entirely correct assumption. The power system is a quasi-static system and thus changes slowly with time [2]. Not only do the system states change with time, but also the line parameters are to some extent time variant. Occurrences such as weather, temperature effects and aging of lines all affect the parameter values in some extent over time. Moreover, the initially calculated parameter values may in fact differ from the actual values, and studies have found that the values may vary from the actual ones in the order of 5 % [3].

The model that the SE is based on could itself also be a source of reduced accuracy. The general model that is generally used is slightly simplified and assumes fully symmetric loads and a perfectly transposed grid. Furthermore, the simplification of using the so called π-model with lumped values of the capacitance may also reduce the accuracy, and especially for longer line sections. Thus, the assumption that the line model and line parameters are perfectly known is not true. Large measurement errors can be detected even if line parameters are not correct. However, in order to find small measurement errors and estimate the size of those errors, the estimation has to be very accurate. The need of an accurate SE is thus obvious and in order to increase the reliability of the results from the estimation, the impact of these discrepancies needs to be examined.

A possible, yet somewhat unused, method of increasing the accuracy of the SE is to include the estimation of suspected erroneous line parameters within the actual state estimation. By this approach, the impact of erroneous line parameters could be decreased and the total accuracy of the estimation increased. This method of parameter estimation (PE) is still generally not adopted by system operators and the possibilities and challenges of the method are to a large extent still not investigated. Previous studies have shown that PE based on augmentation of the state vector and using Kalman filtering is one of the most accurate parameter estimation algorithms that is present today [4].

1.1.1 Measurement requirements in the Swedish power grid

The accuracy requirements of the energy measurement systems in the Swedish power grid are regulated from the Swedish government authority called the Swedish Board for Accreditation and Conformity Assessment (SWEDAC) [5]. The requirements on the accuracy of the measurement devices are depending on the power system level. For example, in the case of the Swedish transmission grid, the accuracy of in principal all energy measurement devices have to be in in the range of $\pm$ 0.5 % [5].

According to regulations from SWEDAC, a periodic inspection is required for all energy measuring systems used in operation within the Swedish grid [5]. The operation of the measuring system and the largest error has to continuously meet the stated requirements. This requirement is ensured by period inspections with a largest interval fixed to 6 years. In between these inspection intervals, a continuous monitoring of the system is also performed.

By developing and using statistical analysis of these measurements, a continuous supervision of the requirements could be possible without even performing an actual inspection. If the reliability of these statistical analyses would be sufficiently high, it could potentially be developed into an accredited method of supervising measurement infrastructure. The application of using the results from a SE has been proposed as one of the methods that potentially could be used for the continuous supervision of the measurement infrastructure.

1.2 Review of previous studies

The previous studies covering PE is somewhat limited and actual field testing of the method is close to non-existent. One of the first studies dedicated to PE by using Kalman filtering is found in [6] where an experimental set of parameter errors in the range of 3-10 % is analysed. The estimation used generated noisy measurement data in a 24-bus large network and the results show that after a few filtering cycles, the estimated parameters are very close to the actual values. However, the parameters are treated as constants, thus limiting the PE algorithm flexibility to parameter variations due to, for example, corona losses or temperature changes. Furthermore, there is no information provided on the noise and measurement levels associated with the measurement samples. If there are no added linear measurement errors introduced, the parameter estimation will always be perfect, and it is therefore hard to evaluate the results of this report.

The PE algorithm with Kalman filtering is further tested in [7] where time varying parameters are dealt with for the first time. Once again, a large network is being tested with very accurate results obtained. However, all measurement data is once again generated with added noise, and there thus is no actual real-life data tested. Therefore, a simulation if it was feasible to follow the small time variations of the parameters due to external impacts, such as weather conditions, was not performed. Yet again, there is no information provided regarding the noise and/or error magnitudes on the generated data and it is thus hard to evaluate the results.

Another report [8], which is not fully dedicated to the PE problem, examines a large network containing three separated branches with erroneous series impedance. While the parameter errors are significantly reduced by the implemented PE, several relative errors remain high in the estimation. Moreover, in this report, no information is presented on the applied measurement accuracy.

Another report examines the possibilities of using the PE algorithm to estimate the transformer tap position [9] by using the so called residual sensitivity analysis method. Variable transformer tap positions may be modelled as dynamic parameters and significant errors may be experienced if these are not taken under consideration. The report examines the possibilities of this method and the results are found to be promising. Several other reports cover related topics such as parameter estimation using normal equations or residual sensitivity analysis.

The effect that parameter errors have on the output of the SE is examined in [10]. The study examines a large network, with both parameter errors and errors in the transformer tap settings implemented in the system. The results show that erroneous parameters may affect the calculation of unmeasured line flow power levels significantly. The results are however only presented for the lines with no voltage or power flow measurements in either end of the line. Since these lines are unmeasured, the estimation is bound to be less accurate than for a measured line.

1.3 Aim of thesis

The main goal of the following thesis may be divided into two separate, yet interconnected, parts.

- **Parameter and model errors sensitivity:** The first objective is to determine the impact that parameter and model errors may have on the accuracy of the SE. The aim is thus to determine which errors that are related to parameter and model errors, and which errors that are related to measurement errors. Furthermore, in order to detect errors within the measurement infrastructure, the uncertainty due to parameter and model errors has to be estimated. The report will thus further strive to develop tools and methods for estimating the largest error that may be caused by errors in the model.
- **Feasibility of using parameter estimation to increase accuracy of state estimation:** The second main objective is to determine the possibilities of increasing the accuracy of the SE by introducing parameter estimation within the ordinary estimation model. Thus, if parameter errors are present, the objective is to examine during what conditions it is feasible to estimate more accurate values for the parameters. The parameter estimation method is then verified by using actual measurement data from a part of the Swedish transmission grid.

1.4 Scope

The impact of parameter errors is examined both for the case of a single branch and for a larger 4-bus network. Simulations of different combinations of parameter errors and power flow states are time demanding, and a few selected simulations will instead be performed. The model errors are only examined for the case of poorly transposed transmission lines. Thus, estimation errors due to simplifications such as the π-model or the neglected conductance to earth will not be investigated.

The report will use the so called augmented state estimation algorithm to estimate parameters. There are a number of other methods available, each with its specific advantages and disadvantages. However, the augmented state estimation with Kalman filtering is generally found to be one of the most accurate methods available for time series data [11]. Since a high accuracy is of high importance in the project, this model is found to be superior. Furthermore, simulations within the report will be constructed by using long line corrected parameter values and the so called π-model. This is the most common model that is being used for SE and no other models will thus be examined.

Moreover, the feasibility of using parameter estimation is only performed for the single-branch and not in the case of a network.

1.5 Thesis structure

The report is principally divided into several separate, although interconnected, parts. The first theory section covers the power system modelling and the adopted assumptions for the three-phase model as well as for the transition to the single-phase model. Next is a section that briefly discusses the basics of state estimation and bad data identification, followed by a section that introduces the theory of parameter estimation. This background and theory is later used to aid the comprehension and put the results into a context.

The method and simulations parts introduce the reader to the examined simulations and discuss why that specific approach has been chosen. The simulations and the models are constructed and the used data is presented. The result for each case is then presented and is briefly explained within each separate result section. Finally, the results are analysed and discussed and conclusions for the project are made. In the appendixes the measured grid data used in the simulations is presented along with the parameter values for the chosen grid configurations.

2 Power system modelling and assumptions

The power system is generally assumed to be operating in steady state with perfectly balanced conditions. This indicates that branch power flows and bus loads are three phased and perfectly balanced, all transmission lines are perfectly transposed, and occurring shunt devices are symmetrical in all three phases [11]. In the case when all these conditions are fulfilled, the system can be modelled solely by the positive sequential components. Furthermore, the parameters of the system are assumed to be constant and fully known.

In order to estimate the impact of non-balanced conditions on the accuracy of the SE, the equivalent single phase model has to be extended into the actual three-phase model. The following section examines the theory of the three phase model and the origins of parameter and model errors.

2.1 Three-phase transmission model

Transmission lines with a length of less than 250 km are generally represented by the so called π-model [12]. The π-model assumes that the total line charging susceptance can be modelled as lumped values in each end of the lines. The conductance to earth is commonly very small and is in general neglected.

In Figure 1, the π-model for all three phases of a transmission line is shown as well as the ground plane. The figure illustrates the self-impedance (Z_{11}, Z_{22}, Z_{33}), as well as the mutual line impedance between the phases $(Z_{12}, Z_{13}, Z_{21}, Z_{23,} Z_{31}, Z_{32})$. Furthermore, the line charging susceptance between the phases is illustrated $\left(Y_{12}, Y_{13}, Y_{21}, Y_{23,} Y_{31}, Y_{32}\right)$ as well as the charging susceptance to ground (Y_{11}, Y_{22}, Y_{33}). All charging susceptance values are modelled as lumped values in each end of the lines.

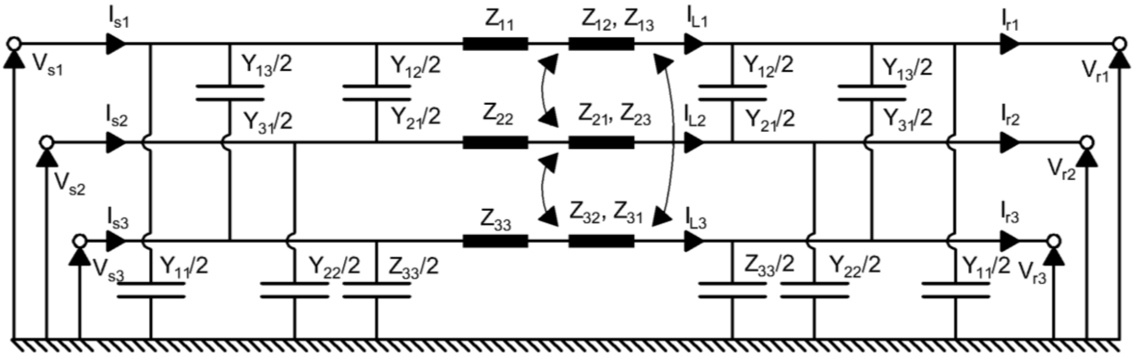

Figure 1. Illustration of a three-phase π-model with all the mutual- and self-impedances present

The line impedance and line charging matrices may be stated as

$$Z_M = \begin{bmatrix} Z_{11} & Z_{12} & Z_{13} \\ Z_{21} & Z_{22} & Z_{23} \\ Z_{31} & Z_{32} & Z_{33} \end{bmatrix} \tag{2.1}$$

$$Y_M = \begin{bmatrix} Y_{11} & Y_{12} & Y_{13} \\ Y_{21} & Y_{22} & Y_{23} \\ Y_{31} & Y_{32} & Y_{33} \end{bmatrix} \tag{2.2}$$

In order to analyse the behaviour of the three-phase model, an expression for how voltages and currents in the sending end affects the voltages and currents in the receiving end is required. The following theory section is developed by the author of the report, with aid of the conventional analysis of the single-phase model. For reference to this model, the reader is referred to [13].

By studying Figure 1 and using the matrices (2.1) and (2.2) the following expression for the line current in the first phase, I_{L1} may be found

$$I_{L1} = I_{r1} + \left(\frac{Y_{11}}{2} \cdot V_{r1} + \frac{Y_{12}}{2} \cdot V_{r2} + \frac{Y_{13}}{2} \cdot V_{r3}\right) \tag{2.3}$$

The line currents of the other phases may be expressed in a similar way

$$I_{L2} = I_{r2} + \left(\frac{Y_{21}}{2} \cdot V_{r1} + \frac{Y_{22}}{2} \cdot V_{r2} + \frac{Y_{23}}{2} \cdot V_{r3}\right) \tag{2.4}$$

$$I_{L3} = I_{r3} + \left(\frac{Y_{31}}{2} \cdot V_{r1} + \frac{Y_{32}}{2} \cdot V_{r2} + \frac{Y_{33}}{2} \cdot V_{r3}\right) \tag{2.5}$$

By using vector-matrix form, these equations may be rewritten more compactly as

$$\begin{bmatrix} I_{L1} \\ I_{L2} \\ I_{L3} \end{bmatrix} = \begin{bmatrix} 1 & 0 & 0 \\ 0 & 1 & 0 \\ 0 & 0 & 1 \end{bmatrix} \begin{bmatrix} I_{r1} \\ I_{r2} \\ I_{r3} \end{bmatrix} + \frac{1}{2} \begin{bmatrix} Y_{11} & Y_{12} & Y_{13} \\ Y_{12} & Y_{22} & Y_{23} \\ Y_{13} & Y_{23} & Y_{33} \end{bmatrix} \begin{bmatrix} V_{r1} \\ V_{r2} \\ V_{r3} \end{bmatrix} \tag{2.6}$$

Eq. (2.6) may be further simplified by using a more general notation as

$$[I_L] = [I_{MAT}][I_r] + \frac{1}{2}[Y_M][V_r] \tag{2.7}$$

where $[I_{MAT}]$: 3×3 large identity matrix

By then using Kirchhoff's laws, the voltage in the sending end may be expressed as

$$V_{s1} = V_{r1} + (Z_{11} \cdot I_{L1} + Z_{12} \cdot I_{L2} + Z_{13} \cdot I_{L3}) \tag{2.8}$$

In the same way as in (2.7) all phase voltages may be rewritten in the more compact vector-matrix form as followed

$$[V_s] = [I_{MAT}][V_r] + [Z_M][I_L] \tag{2.9}$$

By then substituting the expression from (2.7) into (2.9), the following expression for the sending end voltages may be found

$$[V_s] = [I_{MAT}][V_r] + [Z_M]\left[[I_{MAT}][I_r] + \frac{1}{2}[Y_M][V_r]\right] \tag{2.10}$$

By using matrix multiplication and gathering the terms with respect to $[V_r]$ and $[I_r]$ the following expression may be found

$$[V_s] = \left([I_{MAT}] + \frac{[Z_M][Y_M]}{2}\right)[V_r] + [Z_M][I_r] \tag{2.11}$$

The same method is then used to calculate the currents of the sending end

$$[I_s] = [I_L] + \left[\frac{Y_M}{2}\right][V_s] \tag{2.12}$$

By then substituting the expressions of (2.7) and (2.11) into (2.12), the following expression may be found

$$[I_s] = [I_{MAT}][I_r] + \frac{1}{2}[Y_M][V_r] + \left[\frac{Y_M}{2}\right]\left(\left([I_{MAT}] + \frac{[Z_M][Y_M]}{2}\right)[V_r] + [Z_M][I_r]\right) \tag{2.13}$$

By once again gathering the terms with respect to $[V_r]$ and $[I_r]$ the following expression may be found

$$[I_s] = [Y_M]\left([I_{MAT}] + \frac{[Z_M][Y_M]}{4}\right)[V_r] + \left([I_{MAT}] + \frac{[Z_M][Y_M]}{2}\right)[I_r] \tag{2.14}$$

The equivalent $ABCD$-matrix for the three phase model that is commonly used for the single phase model may thus be stated as followed

$$A = [I_{MAT}] + \frac{[Z_M][Y_M]}{2} \tag{2.15}$$

$$B = [Z_M] \tag{2.16}$$

$$C = [Y_M]\left([I_{MAT}] + \frac{[Z_M][Y_M]}{4}\right) \tag{2.17}$$

$$D = [I_{MAT}] + \frac{[Z_M][Y_M]}{2} \tag{2.18}$$

The above stated equations for the three phase model are thus similarly stated as for the equivalent single phase model. The relationship between the sending and receiving end voltages and currents may thus be formulated as followed

$$\begin{bmatrix} V_s \\ I_s \end{bmatrix} = \begin{bmatrix} A & B \\ C & D \end{bmatrix} \begin{bmatrix} V_r \\ I_r \end{bmatrix} \tag{2.19}$$

Note that (2.19) contains information of all three phases and that $\begin{bmatrix} V_s \\ I_s \end{bmatrix}$ is thus a 6×1 matrix. In order to calculate the active and reactive power, voltage drop etc. the same method as in the classical single-phase model is used. The effect and simulation of an unbalanced grid is analysed in section 5.1 and the results are presented in section 6.1.

2.2 Equivalent single-phase model

The three-phase model developed in the previous section may in the event of complete symmetric conditions be reduced into an equivalent single-phase model [13]. This is achieved by initially transforming all phase voltages and phase currents, as well as the impedance and admittance matrices into so called symmetric components. Any unbalanced or balanced three-phase system may be expressed as the sum of the symmetrical sequence vectors; the positive, the negative, and the zero sequence vectors [13]. The transformation between phase values and symmetric components is performed by using the transformation matrix and its inverse, written as

$$A = \begin{bmatrix} 1 & 1 & 1 \\ 1 & a^2 & a \\ 1 & a & a^2 \end{bmatrix} \tag{2.20}$$

$$A^{-1} = \frac{1}{3}\begin{bmatrix} 1 & 1 & 1 \\ 1 & a & a^2 \\ 1 & a^2 & a \end{bmatrix} \tag{2.21}$$

where a : complex number with the value of $e^{\frac{+j2\pi}{3}} = (-0.5 + j0.866)$

If a fully symmetric three-phased voltage is assumed, the symmetric components may be calculated by multiplying the phase values of the voltage with (2.21) as follows [13]

$$\begin{bmatrix} V_0 \\ V_1 \\ V_2 \end{bmatrix} = \frac{1}{3}\begin{bmatrix} 1 & 1 & 1 \\ 1 & a & a^2 \\ 1 & a^2 & a \end{bmatrix}\begin{bmatrix} Ve^{j(\omega t+\varphi)} \\ Ve^{j(\omega t+\varphi-\frac{2\pi}{3})} \\ Ve^{j(\omega t+\varphi+\frac{2\pi}{3})} \end{bmatrix} = \begin{bmatrix} 0 \\ Ve^{j(\omega t+\varphi)} \\ 0 \end{bmatrix} \tag{2.22}$$

where V_0 : zero sequence voltage

V_1 : positive sequence voltage

V_2 : negative sequence voltage

$Ve^{j(\omega t+\varphi+x)}$: corresponding phase voltage

From (2.22) it is possible to see that during perfectly symmetric conditions, the symmetric components consist solely of the positive-sequence component. The exact same method may then be used in order to derive the symmetric components for the current. Following, the voltage drop over an impedance matrix as it is defined in (2.1) may in compact matrix form be expressed as

$$[V_{a-c}] = [Z_M]\,[I_{a-c}] \tag{2.23}$$

where V_{a-c} : phase voltages in matrix form

I_{a-c} : phase currents in matrix form

By transforming the phase voltages and the phase currents into symmetric components using (2.22) it is possible to rewrite (2.23) into symmetric components

$$[V_{0-1-2}] = [A^{-1}]\,[Z_M]\,[A]\,[I_{0-1-2}] \tag{2.24}$$

where V_{0-1-2} : symmetric component matrix of the voltage

I_{0-1-2} : symmetric component matrix of the current

Finally, the impedance matrix Z_M may be transformed into symmetric components by definying it as

$$Z_{0-1-2} = [A^{-1}]\,[Z_M]\,[A] \tag{2.25}$$

In the case of an asymmetric line, Z_M will be a full matrix with different values in most fields [13]. However, in the case of a symmetric and fully transposed line, it is possible to show that the elements in Z_M are related as

$$Z_{11} = Z_{22} = Z_{33} = Z_s \tag{2.26}$$

$$Z_{12} = Z_{21} = Z_{31} = Z_d \tag{2.27}$$

giving Z_M the following structure

$$Z_M = \begin{bmatrix} Z_s & Z_d & Z_d \\ Z_d & Z_s & Z_d \\ Z_d & Z_d & Z_s \end{bmatrix} \tag{2.28}$$

By then using (2.25), the impedance matrix in symmetrical components may be simplified into

$$Z_{0-1-2} = \begin{bmatrix} Z_s + 2Z_d & 0 & 0 \\ 0 & Z_s - Z_d & 0 \\ 0 & 0 & Z_s - Z_d \end{bmatrix} \tag{2.29}$$

The positive sequence impedance has thus the value of $Z_s - Z_d$. The exact same methodology may be used in order to transform the admittance matrix Y_M into symmetric components. From (2.22) it was found that both symmetric voltages and currents may be expressed solely by using the positive sequence component. Hence, if the power system is operating with symmetric conditions, calculations with the positive sequence components of the line voltages, currents, and impedances are found to be sufficient. The single-phase model may be derived similarly as for the three-phase model, but instead only using the positive sequence components. Thus, using the same methodology, an equivalent $ABCD$-matrix may be formed for the single-phase model.

2.3 Origin of model errors and parameter errors

Model errors origins from the fact that the provided and used model is insufficient to explain the actual conditions of the transmission lines. The equivalent single phase model is only fully valid in the case of a fully balanced load and fully transposed transmission lines. If these conditions are not met, the three-phase model explained in section 2.1 could be preferred if a per-phase analysis is needed. Furthermore, the π-model itself is a simplified model and the lumped capacitances is a simplification which is only valid with sufficiently high accuracy for line lengths shorter than about 250 km. In order to achieve a more accurate solution the exact effect of the distributed parameters must be considered [13]. The distributed parameters, namely the ABCD parameters of the equivalent π-model for a long line, are thus calculated and these corrected long line parameters are then used as an input for the SE. The long line corrected parameters will always have a small conductance to earth that models the no-load losses of the line. However, this conductance is generally neglected within the SE model and albeit having a small value it could affect the results of the estimation.

Parameter errors origins from the fact that the calculated parameter values differ from the actual ones for several different reasons. Previous studies have shown that parameter data provided by manufacturers may differ up to 5 % in many cases. The line length estimation may also in some cases be performed poorly, which would result in erroneous parameter values [3]. Other reasons such as non-updated network changes or mutual inductance due to near lying power lines may also affect the parameter values used in the SE.

As was previously mentioned, the power system is operating in a quasi-static state. However, not only does the system states change with time, but the line parameters are also in some magnitude time variant [3]. Temperature variations will primarily affect the line resistance, but since the sag of the line changes with temperature, the shunt capacitance and to some extent the inductance, will also be affected. Moreover, certain environmental conditions may cause phenomenon such as corona which will significantly affect aspects such as the line losses of the power system. Ageing of lines is a slower process but may also affect the parameter values to some extent.

3 State Estimation

State estimation is the concept of obtaining the best estimation of the actual state within the grid by using an over-determined system with imperfect measurements. The state variables in a power system are the voltage magnitudes and the relative phase angles at the system nodes. The SE in combination with redundant measurements reduces the impact of large errors and finds the most optimal estimate of the system [11]. The most commonly used criterion of the optimal estimate is that of minimizing the sum of the squares of the differences between the estimated and the measured values [14].

Power system operations such as system security control and economic dispatch requires that the system performance is estimated on a regular basis. However, due to the fact that measurements always will be related with both some magnitude of noise and systematic measurement errors, an accurate estimation is the key to well-functioning power system operation. The magnitude of the measurement errors is not only dependent on the accuracy of the equipment, but also systematic errors such as nonlinearities of current and voltage transformers or time and environment dependencies.

The following section briefly covers the theoretical background of SE. The literature covering SE is quite extensive and a there are several methods formulated such as optimization of the algorithm and observability analysis. However, this section is mainly focused on presenting the basic background of the algorithm as well as the system measurement functions. The theory of the following section is gathered mainly from [11] unless specifically stated otherwise. Hence, if more depth regarding the theory of power system state estimation is desired, the reader is referred to that reference.

3.1 Weighted Least Squares Estimation

The goal with the SE is to determine the most probable state of the system based on a redundant amount of measurements. One way to achieve the goal is to use the so called maximum likelihood estimation (MLE) [11]. If the measurement errors are expected to have a known probability distribution with unknown parameters, then the joint probability function for all measurements in the system can be stated as a function of these unknown parameters. The joint probability function will attain the highest value when the unknown parameters are chosen to values closest to their actual values. The optimization of this function will then result in the maximum likelihood estimates of the measurements. The Gaussian, or the Normal, probability density function (PDF) for a random measurement z can defined as [15]

$$f(z) = \frac{1}{\sigma\sqrt{2\pi}} e^{-\frac{1}{2}\left(\frac{z-\mu}{\sigma}\right)^2} \tag{3.1}$$

where σ : standard deviation of z

μ : expected or mean value of $z = E(z)$

A plot of the PDF is illustrated in Figure 2. The figure shows the probability of a measurement attaining a certain value. Note that the standard deviation will provide a measure of the probability and seriousness of measurement errors [14]. If σ is small, the measurement is generally not affected as much by noise (i.e. higher quality measurement device), whereas a large value of σ is related with larger measurement noise levels (i.e. lower quality measurement device).

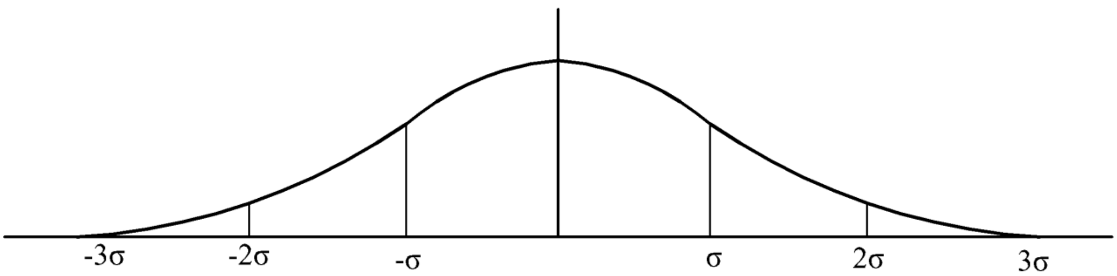

Figure 2. Probability density function for a normal distributed measurement

By assuming that the normal probability density function is equal for all measurements and that the measurement errors are non-dependent of each other, the joint probability function for m independent measurements can be expressed as the product of each individual probability density function. The joint probability function can thus be stated as

$$f_m(z) = f(z_1)f(z_2) \ldots f(z_i) \tag{3.2}$$

where z_i : number of measurements

$f_m(z)$: standard deviation of z

The objective of the probability of the MLE is then to maximize the joint probability function by varying the parameters; in this case the mean and the variance of each density function. In order to determine these parameters, the function is generally replaced by the equivalent logarithm to simplify the optimization procedure. This adjusted function is generally denoted as the Log-Likelihood Function and may be stated as

$$\begin{aligned}\mathcal{L} = \log f_m(z) &= \sum_{i=1}^{m} \log f(z_i) \\ &= -\frac{1}{2}\sum_{i=1}^{m} \log\left(\frac{z_i - \mu_i}{\sigma_i}\right)^2 - \frac{m}{2}\log(2\pi) - \sum_{i=1}^{m} \log \sigma_i\end{aligned} \tag{3.3}$$

The MLE procedure will then maximize the function in (3.3) by solving the following problem

$$minimize \quad \sum_{i=1}^{m} \log\left(\frac{z_i - \mu_i}{\sigma_i}\right)^2 \tag{3.4}$$

This equation can be simplified and rewritten in the terms of the residual r_i of the i-th measurement, as followed

$$r_i = z_i - \mu_i = z_i - E(z_i) \tag{3.5}$$

where the mean value or the expected value $E(z_i)$ may be expressed as the nonlinear function $h_i(x)$ that relates the state vector x to the i-th measurement. The measurement value for the i-th measurement may thus be stated as

$$h_i(x) = \mu_i = E(z_i) \tag{3.6}$$

The square of each residual is weighted by the matrix $W_i = \sigma_i^{-2}$ which is thus the inversely related to the assumed error variance for each measurement. Thus, the minimization of (3.5) is achieved by minimizing the sum of the squares of the product of residuals and the weighting matrix as followed

$$\text{minimize} \quad \sum_{i=1}^{m} W_i\, r_i^2 \tag{3.7}$$

$$\text{with respect to} \qquad z_i = h_i(x) + r_i, \quad i = 1,2,\dots,m. \tag{3.8}$$

The optimized solution to the above stated problem is called the weighted least squares (WLS) estimator for x and is the key parts of the SE procedure.

3.1.1 State estimation using WLS algorithm

The SE procedure using the WLS algorithm is reviewed in this section and the theory is mainly gathered from [11]. A set of measurements given by the vector z, assumed to be expressed by the non-linear function of the state vectors and a vector of measurement errors, can be stated in compact matrix form as

$$z = \begin{bmatrix} z_1 \\ z_2 \\ \vdots \\ z_m \end{bmatrix} = \begin{bmatrix} h_1(x_1, x_2, \dots, x_n) \\ h_2(x_1, x_2, \dots, x_n) \\ \vdots \\ h_m(x_1, x_2, \dots, x_n) \end{bmatrix} + \begin{bmatrix} e_1 \\ e_2 \\ \vdots \\ e_m \end{bmatrix} = h(x) + e \tag{3.9}$$

where z_m : number of measurements

x_n : number of states defining the measurement

e_m : number of related measurement errors

As discussed previously, the measurements are assumed to be fully independent of each other, and the measurement errors are thus also independent. The covariance matrix R_{ii} is thus fully diagonal, i.e. $R_{ii} = diag\{\sigma_1^2, \sigma_1^2, \dots, \sigma_m^2\}$.

The weighted least squares estimator will then minimize the following function

$$J(x) = \sum_{i=1}^{m} \frac{\left(z_i - h_i(x)\right)^2}{R_{ii}} = [z - h(x)]^T R^{-1} [z - h(x)] \tag{3.10}$$

In order to minimize the above stated objective function, the first-order optimality conditions will have to be fulfilled. These may be stated as

$$g(x) = \frac{\partial J(x)}{\partial x} = -H^T(x) \cdot R_{ii}^{-1}[z - h(x)] = 0 \tag{3.11}$$

where $H(x)$ is the Jacobian of state vector function, defined as

$$H(x) = \left[\frac{\partial h(x)}{\partial x}\right] \tag{3.12}$$

An expansion of $g(x)$ into the first order of the Taylor series yields the following expression

$$g(x) = g(x^k) + G(x^k)(x - x^k) \tag{3.13}$$

Using this first order term of the Taylor series leads to an iterative solution scheme commonly denoted as the Gauss-Newton method. This may then be stated as

$$x^{k+1} = x^k - [G(x^k)]^{-1} \cdot g(x^k) \tag{3.14}$$

where
- k : iteration index
- x^k : state vector at iteration k
- $g(x^k)$: first order optimality condition at iteration k
- $G(x^k)$: gain matrix

The gain matrix is commonly positive definite, sparse, and symmetrical and is defined as

$$G(x^k) = \frac{\partial g(x^k)}{\partial x} = H^T(x^k) \cdot R_{ii}^{-1} \cdot H(x^k) \tag{3.15}$$

The solution is thus found by iteratively solving (3.14) until sufficient accuracy is reached.

3.2 System measurement functions

The system measurements consist generally of conventional power flow and voltage measurements, but in some cases other measurements such as current magnitude or phasor measurements are present [11]. The output of the common SE is then generally the steady state bus voltage phasors, as these together with the network model is sufficient for determination of the operating conditions of the power system. These measurements may be expressed implicitly by the system states in either polar or rectangular form. Assuming that the simple two-port π-model is sufficient to model the network branches, the following expressions may be formulated for the most common measurements.

- Active and reactive power flow from bus i and j

$$P_{ij} = V_i^2\left(g_{si} + g_{ij}\right) - V_i V_j (g_{ij} \cos\theta_{ij} + b_{ij} \sin\theta_{ij}) \tag{3.16}$$

$$Q_{ij} = -V_i^2\left(b_{si} + b_{ij}\right) - V_i V_j (g_{ij} \sin\theta_{ij} - b_{ij} \cos\theta_{ij}) \tag{3.17}$$

where V_i and V_j : voltage magnitude at buses i and j

θ_{ij} : phase angle difference between buses i and j

g_{ij} and b_{ij} : admittance of the series branch connecting the buses

g_{si} and b_{si} : admittance of the shunt branch connected at bus i

- Total active and reactive power injection at bus i

$$P_i = V_i \sum_{j=1}^{N} V_j \left(G_{ij} \cos\theta_{ij} + B_{ij} \sin\theta_{ij}\right) \tag{3.18}$$

$$Q_i = V_i \sum_{j=1}^{N} V_j \left(G_{ij} \sin\theta_{ij} - B_{ij} \cos\theta_{ij}\right) \tag{3.19}$$

where G_{ij} and B_{ij} : ijth element of the bus admittance matrix

N : number of buses that are directly connected to bus i

Since voltage is defined as a system state, the bus voltage measurements are simply defined by the respective state value. The measurement Jacobian is based on the partial derivative of all the measurement functions and will have the following structure

$$H = \begin{bmatrix} \frac{\partial P_{inj}}{\partial \theta} & \frac{\partial P_{inj}}{\partial V} \\ \frac{\partial P_{flow}}{\partial \theta} & \frac{\partial P_{flow}}{\partial V} \\ \frac{\partial Q_{inj}}{\partial \theta} & \frac{\partial Q_{inj}}{\partial V} \\ \frac{\partial Q_{flow}}{\partial \theta} & \frac{\partial Q_{flow}}{\partial V} \\ 0 & \frac{\partial V_{mag}}{\partial V} \end{bmatrix} \tag{3.20}$$

The expressions for each partial derivative may then be stated as followed [11]:

- Partial derivatives corresponding to real power injection measurements

$$\frac{\partial P_i}{\partial \theta_i} = V_i \sum_{j=1}^{N} V_j \left(-G_{ij} \sin \theta_{ij} + B_{ij} \cos \theta_{ij}\right) - V_i^2 B_{ii} \tag{3.21}$$

$$\frac{\partial P_i}{\partial \theta_j} = V_i V_j (G_{ij} \sin \theta_{ij} - B_{ij} \cos \theta_{ij}) \tag{3.22}$$

$$\frac{\partial P_i}{\partial V_i} = \sum_{j=1}^{N} V_j \left(G_{ij} \cos \theta_{ij} + B_{ij} \sin \theta_{ij}\right) + V_i G_{ii} \tag{3.23}$$

$$\frac{\partial P_i}{\partial V_j} = V_i (G_{ij} \cos \theta_{ij} + B_{ij} \sin \theta_{ij}) \tag{3.24}$$

- Partial derivatives corresponding to real power flow measurements

$$\frac{\partial P_{ij}}{\partial \theta_i} = V_i V_j (g_{ij} \sin \theta_{ij} - b_{ij} \cos \theta_{ij}) \tag{3.25}$$

$$\frac{\partial P_{ij}}{\partial \theta_j} = -V_i V_j (g_{ij} \sin\theta_{ij} - b_{ij} \cos\theta_{ij}) \tag{3.26}$$

$$\frac{\partial P_{ij}}{\partial V_i} = -V_j (g_{ij} \cos\theta_{ij} + b_{ij} \sin\theta_{ij}) + 2V_i\big(g_{ij} + g_{si}\big) \tag{3.27}$$

$$\frac{\partial P_{ij}}{\partial V_j} = -V_i (g_{ij} \cos\theta_{ij} + b_{ij} \sin\theta_{ij}) \tag{3.28}$$

- Partial derivatives corresponding to reactive power flow measurements

$$\frac{\partial Q_{ij}}{\partial \theta_i} = -V_i V_j (g_{ij} \cos\theta_{ij} + b_{ij} \sin\theta_{ij}) \tag{3.29}$$

$$\frac{\partial Q_{ij}}{\partial \theta_j} = V_i V_j (g_{ij} \cos\theta_{ij} + b_{ij} \sin\theta_{ij}) \tag{3.30}$$

$$\frac{\partial Q_{ij}}{\partial V_i} = -V_j (g_{ij} \sin\theta_{ij} - b_{ij} \cos\theta_{ij}) - 2V_i\big(b_{ij} + b_{si}\big) \tag{3.31}$$

$$\frac{\partial Q_{ij}}{\partial V_j} = -V_i (g_{ij} \sin\theta_{ij} - b_{ij} \cos\theta_{ij}) \tag{3.32}$$

- Partial derivatives corresponding to voltage magnitude measurements

$$\frac{\partial V_i}{\partial \theta_i} = 0, \qquad \frac{\partial V_i}{\partial \theta_j} = 0, \qquad \frac{\partial V_i}{\partial V_i} = 1, \qquad \frac{\partial V_i}{\partial V_j} = 0 \tag{3.33}$$

Since the voltage magnitude is defined as a state within the estimation model, the partial derivative of the voltage with respect to phase angles and other bus voltages will always be equal to zero. Both the measurement functions and the Jacobian will of course be extended in the case other measurements such as current magnitude or phasor measurements are available.

3.3 Bad data identification

Although the SE algorithm is intended to filter out and reduce the impact of bad measurement data, this impact may still affect the results of the SE significantly [11]. One method of reducing this impact is to identify and eliminate these large measurement errors. Small random errors, or noise, are always to some extent present in the system due to the finite accuracy of meters and connected communication systems. Larger errors may instead occur when the metering systems have faults such as biases, drifts, or linear errors. The SE may also be misled by incorrect parameter values which will consequently be detected as bad measurements by the SE. This impact is further explained in section 4.3.

The treatment of the erroneous measurements depends on the method of SE. Since the conventional WLS method for the SE algorithm is used within the report, the bad data detection algorithm that is associated with this method will also be examined. The detection and identification of bad data is in this case performed after the estimation process by assessing the measurement residuals.

3.3.1 Properties of measurement residuals

Considering a linearized measurement equation where the Δ illustrates the change between two measurement points

$$\Delta z = H\Delta x + e \tag{3.34}$$

where the mean value of the error e is equal to zero, and the covariance of the error is $cov(e) = R$, which is the diagonal matrix based on the assumption that the errors of all measurements are not correlated. By using the theory developed in the previous sections, the WLS estimator of the linearized state vector may be stated as followed

$$\Delta x = (H^T R^{-1} H)^{-1} H^T R^{-1} \Delta z = G^{-1} H^T R^{-1} \Delta z \tag{3.35}$$

The estimated value of Δz is then found by using (3.34) and (3.35), as followed

$$\Delta\hat{z} = H\Delta\hat{x} = K\Delta z \tag{3.36}$$

where $\quad K: \quad HG^{-1}H^T R^{-1}$

By using the computed K-matrix it is possible to obtain a crude estimate of the local measurement redundancy around a given meter by examining the corresponding row entries in the matrix. A relatively large diagonal entry compared to the off-diagonal elements implies that the estimated value corresponding to that measurement is mainly determined by the measured value, and hence, the redundancy of that measurement is low. The K-matrix has several specific properties allowing the measurement residuals to be expressed as followed

$$\begin{aligned} r &= \Delta z - \Delta \hat{z} \\ &= (I - K)\Delta z \\ &= (I - K)(H\Delta x + e) \\ &= (I - K)e \\ &= Se \end{aligned} \tag{3.37}$$

where S : residual sensitivity matrix

The derived residual sensitivity matrix, S, represents the sensitivity of the residuals to the measurement errors. By using the specific properties of S and the linear relation found in (3.37), it is possible to state the mean and covariance of the measurement residuals as follows

$$E(r) = E(S \cdot e) = S \cdot E(e) = 0 \tag{3.38}$$

$$Cov(r) = \Omega = SR \tag{3.39}$$

where $E(r)$: mean of measurement residual

$Cov(r)$: covariance of measurement residual

The off-diagonal elements of the residual covariance matrix may then be used to identify significantly interacting measurements on the residuals. Furthermore, the covariance matrix is used significantly in the normalized residuals test which is a common test for bad data detection

3.3.2 Bad data detection by using normalized residuals

There are several methods that can be used for detecting erroneous and bad measurements [11]. A conventional test for detecting bad data is the so called Chi-squares test. However, this test is commonly found to be too inaccurate due to approximations of the residual errors. A more accurate test for finding and detecting bad data is obtained by analysing the normalized residuals. The normalized value of the residual for measurement i can be found by dividing the absolute value of that measurement residual with the corresponding diagonal entry in the residual covariance matrix

$$r_i^N = \frac{r_i}{\sqrt{\Omega_{ii}}} \tag{3.40}$$

The resulting normalized residual vector r^N will then have a standard normal distribution and the largest element in r^N is thus, with high probability, associated with the largest measurement error.

3.3.3 Largest Normalized Residual Test

The bad data detection test using the normalized residuals is generally denoted as the *Largest Normalized Residual Test* (LNRT) [11]. The LNRT is then commonly used for detecting and subsequently removing bad measurement data. The test is composed of the following steps:

1) Perform the WLS estimation and obtain all elements of the measurement residual vector, according to

$$r_i = z_i - h_i(\hat{x}) \tag{3.41}$$

2) Calculate the normalized residuals according to (3.40) for all measurements.
3) Find k such that r_k^N is the largest of all normalized residuals
4) If $r_k^N > C_{threshold}$ then the k-th measurement will be suspected as an erroneous data measurement. $C_{threshold}$ is an arbitrary threshold value chosen according to accuracy preferences.
5) Eliminate the k-th measurement from the data set and re-iterate the WLS estimation once again.

This method is highly accurate in identifying a single bad data measurement. In the case of multiple bad data, alternative methods may be more efficient. The LNRT is also used for the detection and elimination of erroneous parameters and is further discussed in section 4.3.

4 Network parameter estimation

In the case when parameter errors are present it is possible to enhance the SE by introducing parameter estimation [11]. The PE could improve the overall accuracy of the SE and provide better estimates, especially for suspected bad data base values. Inaccurate parameter values may have several undesirable consequences and primarily there will be degradation in the accuracy of the results provided by the SE [11]. It may also affect good measurement values as these might be detected as “bad data” due to a lack of consistency of the network parameters. On the whole, larger parameter errors may result in a reduced confidence in the state estimation results by the system operator and in general result in a higher security margins than necessary. Furthermore, erroneous parameter values will cause the detection and evaluation of erroneous measurement values to become more difficult.

The following section will thus present the concept of parameter estimation. First, the currently used methods and algorithms are presented and discussed. The next section presents the parameter estimation algorithm that is to be applied in this report. Finally, a section discussing the reliability of parameter estimation is introduced. The theory of this section is yet again mainly gathered from [11] unless specifically stated otherwise.

4.1 Influence of parameter errors

The sensitivity of the SE results with respect to parameter errors is obviously of high importance. From a previous study the effect of parameter errors was simulated by examining an IEEE 14-node network at different load flow situations [4]. The simulations assessed how far a single parameter error, in this case the line susceptance, spread over the network. The distances from a branch where the erroneous parameter is found is then considered according to Figure 3. Thus, the measurement at distance 1 refers to the power flow of that particular branch and voltages and power injections of the adjacent buses. The measurement at distance 2 is then compromised of those directly related to measurements at distance 1, and so on.

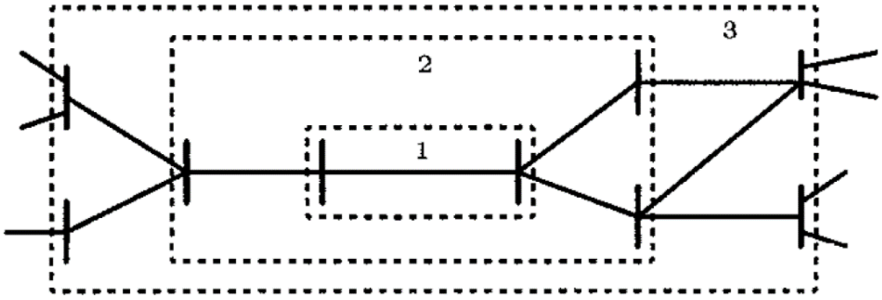

Figure 3. Measurement distance from erroneous branch, reprinted with permission from *[4]*

In the simulation, the actual measurement values were known. The ratio between the averaged estimated measurement error when the line susceptance is erroneous and the same average when the parameter value is correct were then calculated for different magnitudes of parameter error. The results for different distances, as these are defined in Figure 3, is then presented in Figure 4.

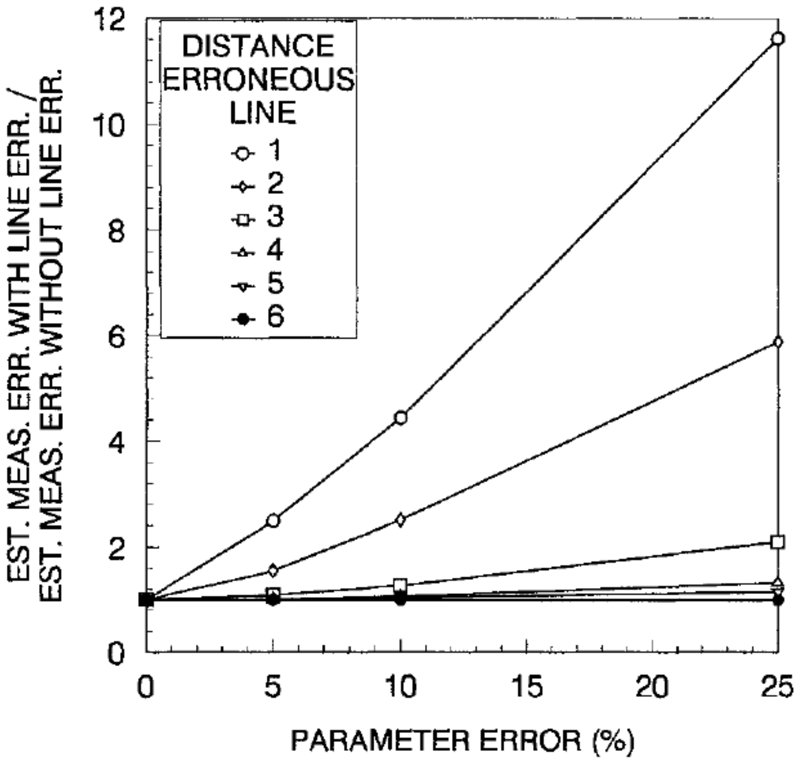

Figure 4. Influence of a single parameter error on estimated measurements at different distances (see Figure 3) from the erroneous line. Reprinted with permission from *[4]*

Several results were obtained from this study. One of the more significant results was that despite a high redundancy of measurements and the fact that only a single parameter is erroneous, a significant deterioration of the accuracy in the SE was found. For a parameter error of 10 % the effect of the error ratio was up to about 4.5 times at a distance of 1 according to Figure 4. The results showed furthermore that the errors decrease significantly with the distance from the erroneous branch, and at a distance equal or larger to 4 the error influence is almost negligible. Moreover, a result which is not found in the figure but may be found in the report is that the parameter error influence is most noticeable when the available measurements have a higher accuracy. A more detailed study of the impact of parameter errors for different grid configurations and measurement redundancies are further examined in detail in simulation 5.2.

4.2 Parameter estimation algorithms

The amount of publications examining the effect of parameter estimation is rather scarce and the estimation problem is therefore not fully examined. There are basically two main methods dedicated for parameter estimation and each has its specific advantages and drawbacks [11]. The methods can be classified as follows:

Residual sensitivity analysis: This estimation methodology is performed after the SE has already been performed and uses the same information that is used to identify suspected erroneous parameters. The main advantage with this method is that the estimation is performed separately from the ordinary SE and there is thus no need to modify the SE code [11].

State vector augmentation: In this method the suspected faulty parameters are included within the state vector [11]. The algorithm will thus estimate both the states and the parameters simultaneously. This method requires a modification of the ordinary SE algorithm to include the parameter estimation. The solution of the state vector augmentation can be achieved by using two different, however related, solving techniques. One solution is based on using normal equations and is basically an extension of the conventional SE model. In order to increase the redundancy and accuracy, several measurements can be used either simultaneously or in sequence.

Another solution of the augmented state vector algorithm is based on Kalman filtering theory [11]. During this approach, arrays of measurement samples are processed sequentially in order to step-by-step improve the accuracy of the parameter estimation. Previous studies have shown that the results from state vector augmentation clearly surpass those based on the residual sensitivity analysis [4]. However, the residual analysis is still required in the process of identifying suspected erroneous parameters. The Kalman filtering method is also found to be preferred to using normal equations if time-varying parameters are estimated [4].

4.2.1 State vector augmentation

Due to the higher level of accuracy, state vector augmentation method will be implemented in this project. In this method the suspected erroneous parameter p is added as an additional state variable [11]. Therefore, the new extended objective function may be stated as

$$J(x,p) = \sum_{i=1}^{m} W_i[z_i - h_i(x,p)]^2 \tag{4.1}$$

where $h_i(x,p)$: new non-linear function that relates the system states *and* the parameter p to the ith measurement

W_i : Weighting matrix which is equal to R_{ii}^{-1}

The parameter p is naturally only affecting the adjacent measurements. Since the initial value of parameter is generally known, a new term can be added to the model in the form of a so called pseudo-measurement. This alters equation (4.1) into

$$J(x,p) = \sum_{i=1}^{m} W_i[z_i - h_i(x,p)]^2 + W_p(p - p_o)^2 \tag{4.2}$$

where W_p : arbitrary weighting factor assigned to the initial parameter value

p_o : initial parameter value

Insufficient research has been conducted on how to choose a value for the weighting factor W_p and it is questioned whether the initial pseudo-measurement should be included or not [11]. If it is not included, it will remove the observability of the parameter and the weighting factor will thus be of no use. This predicament of whether to use or not use an initial pseudo-measurement is however solved by using the Kalman filtering theory which is presented in the following section.

4.2.2 Kalman filtering solution

Kalman filtering is based on an algorithm that uses a series of measurements over time, contaminated by inaccuracies and noise, and produces a more precise estimate of unknown variable [16]. The Kalman filter theory is used to solve the objective function in (4.2) by assuming that at every time sample k, the measurements will be directly related to the states according to

$$z(x) = h(x(k), k, p) + e(k) \tag{4.3}$$

where h now is made dependent on the sample k in order to reflect the quasi-static state of the network parameters from one time sample to the next. By using the initial available parameter vector, p_0, the proposed method is to for each sample k estimate a “better” value of p. This may be formulated as

$$p_{k-1} = p_k + e_p(k) \tag{4.4}$$

where the error vector $e_p(k)$ is assumed similarly as for the measurements to have a zero mean and a fully diagonal covariance matrix $R_p(x)$. The objective function is thus augmented with as many pseudo-measurements as there are suspected parameters and takes the following form

$$J = (p_{k-1} - p_k)^T \cdot R_p^{-1} \cdot (p_{k-1} - p_k) + \ . \ . \ . \tag{4.5}$$

$$+ \sum_{i=1}^{m} [z_i(k) - h_i(x(k), k, p)]^T \cdot W_i \cdot (z_i(k) - h_i(x(k), k, p))$$

This results in the following equation being solved at iteration i of the kth sample, similarly as was the procedure for the ordinary state estimation

$$G^i(k) \begin{bmatrix} \Delta x^i(k) \\ \Delta p_k^i \end{bmatrix} = \begin{bmatrix} H_x^i & H_p^i \\ 0 & I \end{bmatrix}^T \begin{bmatrix} W & 0 \\ 0 & R_p^{-1}(k-1) \end{bmatrix} \begin{bmatrix} z(k) - h\left(x^i(k), k, p_k^i\right) \\ P_{k-1} - p_k^i \end{bmatrix} \tag{4.6}$$

where the gain matrix $G^i(k)$ is

$$G^i(k) = \begin{bmatrix} H_x^i & H_p^i \\ 0 & I \end{bmatrix}^T \begin{bmatrix} W & 0 \\ 0 & R_p^{-1}(k-1) \end{bmatrix} \begin{bmatrix} H_x^i & H_p^i \\ 0 & I \end{bmatrix} \tag{4.7}$$

and H_x^i and H_p^i are the Jacobians of the ordinary state vector function and the state vector function with respect to the suspected parameters. At the end of each iterative process, the covariance matrix of the parameter is updated with the value of

$$R_p(k) = \Lambda_{\text{pp}}(k) \tag{4.8}$$

where $\Lambda_{pp}(k)$ is consisting of the following block of the inverse of the gain matrix

$$G(k)^{-1} = \begin{bmatrix} \Lambda_{\text{xx}}(k) & \Lambda_{\text{xp}}(k) \\ \Lambda_{\text{px}}(k) & \Lambda_{\text{pp}}(k) \end{bmatrix} \tag{4.9}$$

The steps for testing the accuracy of the PE algorithm is tested in section 0 and further analysed in the discussion.

4.3 Identification of suspicious erroneous parameters

In theory it would be possible to estimate all network parameters if a sufficiently long series of fully redundant measurements would be available. However, such estimation would have been computationally cumbersome and it is also found that the parameter error has to be sufficiently large in comparison to the measurement errors for the estimation to be accurate [11]. The identification of erroneous branches and parameters are thus imperative in the estimation process.

The effect that a parameter error will have on an estimated state may be stated mathematically as followed

$$z_s = h_s(x,p) + e_s = h_s(x,p_0) + [h_s(x,p) - h_s(x,p_0)] + e_s \tag{4.10}$$

where p and p_0 again represents the true and erroneous parameters of the network, and where the subscript s is referring to the set of adjacent measurements only. The term within the square brackets in (4.10) may be assumed to be equivalent to an additional measurement error. If this parameter error is then sufficiently large, the term may lead to a bad data being detected and the adjacent measurements will thus have the largest residuals [11]. The corresponding measurement error may be linearized as

$$h_s(x,p) - h_s(x,p_0) \approx \left[\frac{\partial h_s}{\partial p}\right] e_p \tag{4.11}$$

where e_p : parameter error $= p - p_o$

Thus, the branches that are found to have the largest normalized residuals should primarily be declared as suspicious.

4.4 Alternative method of line conductance estimation

The estimation of line conductance may prove to be difficult due to the fact that the magnitude of that parameter is so much smaller than the magnitude of the line susceptance. An alternative method of estimating the line conductance may be to examine the line losses of the single line. Since the line losses have a quadratic relationship to line current, while the measurement errors tend to be linear, it is possible to experimentally estimate the value of the line conductance by examining the relative line losses with respect to the transferred power.

If a short line modelled with only resistance and inductance is considered, the sending and receiving end apparent power in per unit values may be stated as

$$\dot{S}_s = \dot{V}_s \cdot \dot{I}_L{}^* \qquad \dot{S}_r = \dot{V}_r \cdot \dot{I}_L{}^* \tag{4.12}$$

where $\dot{S}_s, \dot{S}_r$: apparent power from the sending and receiving end

$\dot{V}_s, \dot{V}_r$: voltage from the sending and receiving end

$\dot{I}_L{}^*$: line current in conjugate

The reference of the defined apparent power in (4.12) is positive for both the sending end and the receiving end if power is transferred from the sending end to the positive end. The total line losses are then computed by taking the product of the line resistance and the square of the line current

$$P_f = R \cdot |I_L|^2 \tag{4.13}$$

where P_f : line losses

R : line resistance

The relative line losses with respect to the averaged transferred apparent power may then be formulated as

$$P_{f\%} = \frac{R \cdot |I_L|^2}{\left|(\dot{S_s} + \dot{S_r})/2\right|} = \frac{(R \cdot |I_L|^2) \cdot 2}{\left|\dot{V_s} \cdot \dot{I_L}^* + \dot{V_r} \cdot \dot{I_L}^*\right|} \tag{4.14}$$

If the voltage drop over the line is small, the sending and receiving end voltage may be assumed to be equal $V_s \approx V_r$. Then, the magnitude of the relative line losses from (4.14) may be simplified into

$$\left|P_{f\%}\right| \approx \left|\frac{(R \cdot |I_L|^2) \cdot 2}{2V_s I_L}\right| \approx \frac{R}{|V_s|} |I_L| \tag{4.15}$$

Now, the line current may be assumed to have a linear relationship with the apparent power as the voltage level is generally more or less constant within a few percent. Thus, by plotting the relative line losses from (4.15) for a large range of transferred apparent power, a linear relationship may be found with the approximate slope of $\frac{R}{|V_s|}$. Thus, by multiplying (4.15) with the corresponding voltage for all values of transferred power, the slope of the plotted curve is now consisting solely of the line resistance

$$\left|P_{f\%}\right| \cdot |V_s| \approx R \cdot |I_L| \tag{4.16}$$

Naturally, the estimation of the resistance, that is the slope of the plotted curve, will be affected by errors in the measurement infrastructure. Moreover, the slope will also be somewhat affected by the simplification of the line model. The accuracy of this alternative method is examined in section 5.4 for several magnitudes of measurement errors.

5 Methodology and simulations

In the following section, the methodology and the upcoming simulations are thoroughly described and argued for. Initially, the effect of unbalanced grids are analysed in order to see in what conditions the equivalent single-phase model is sufficient. Following is an analysis of the impact that parameter errors may have on the output of the SE model, which is tested for both a single branch and a larger network. Finally, methods of improving the accuracy of the SE are examined. The proposed PE algorithm is investigated and tested for several magnitudes of measurement errors. Moreover, an alternative method of estimating the line resistance is examined.

The power flows and voltages for all simulations are presented in appendix A together with the used line parameters. All simulations and calculations are modelled and calculated by using MATLAB.

5.1 Simulation I: Model error sensitivity analysis

The simulation of model errors is performed by comparing the results of the conventional equivalent single-phase model and the proposed three-phase model for an asymmetric line section. Several magnitudes of line asymmetry are examined and the different combinations of the section lengths and associated transpositions of the line are presented in Table 1. The full impedance and admittance matrix for a typical transmission line configuration, as these are defined from (2.1) and (2.2) are presented below. The values are taken from the sub-application Transmission Line Characteristics Program (TMLC) which is a part of the Siemens based power transmission planning software PSS®E [17]. The actual values are of low importance in this case as the simulation only strives to illustrate the impact of unbalanced grids.

$$Z_M = \begin{bmatrix} 0.0466 + 0.3029\mathrm{i} & 0.0308 + 0.1098\mathrm{i} & 0.0299 + 0.0885\mathrm{i} \\ 0.0308 + 0.1098\mathrm{i} & 0.0478 + 0.2921\mathrm{i} & 0.0308 + 0.1098\mathrm{i} \\ 0.0299 + 0.0885\mathrm{i} & 0.0308 + 0.1098\mathrm{i} & 0.0466 + 0.3029\mathrm{i} \end{bmatrix}$$

$$Y_M = \begin{bmatrix} 5.0895\mathrm{i} & -0.8786\mathrm{i} & -0.2747\mathrm{i} \\ -0.8786\mathrm{i} & 5.3242\mathrm{i} & -0.8786\mathrm{i} \\ -0.2747\mathrm{i} & -0.8786\mathrm{i} & 5.0895\mathrm{i} \end{bmatrix}$$

In the simulation a fully symmetric active load of 0.7 per-unit is connected to the end of the line. The different levels of unbalance are achieved by using a simple, single transmission line with in total three sections. A fully symmetric line would have equal section lengths and this is thus the reference value. The line sections for the different levels of asymmetry are presented in Table 1. For more information regarding how the actual transposition of matrices is performed, the reader is referred to [18]. The voltage and current magnitudes for each phase and for the different levels of asymmetry for the three-phase model are then compared with the case when using the conventional single-phase model.

Table 1. Line sections for different levels of asymmetry

	Section 1 [km]	**Section 2 [km]**	**Section 3 [km]**
High asymmetry	80	20	20
Medium asymmetry	60	30	30
Low asymmetry	50	35	35

The active line losses are also examined for the three-phase model when a transmission line with high asymmetry is analysed. For this simulation, typical measurement data for a single transmission line from Svk is used in order to be able to plot the line losses per phase with respect to the transferred active power. This measurement data is presented in appendix A. The computation of all the three-phase models is performed by using the theory developed in section 2 and by using the ABCD-matrices found in (2.19). The single phased model is computed by using conventional power system calculations which may be found several power system analysis literatures [13]. The results from these simulations is presented in section 6.1 and further discussed in section 7.1.

5.2 Simulation II: Parameter error sensitivity analysis

The effect that parameter errors have on the output of the SE are analysed in the following section. Previous studies have been performed on the accuracy of SE when parameter errors are present, but most studies concentrate on the effect that erroneous parameters has on fully unmeasured lines. In the following simulation, the effect on parameter errors are simulated for the case of full measurements redundancy (voltage and power flow measurements for all buses) and the case for reduced redundancy (voltage measurement for all buses and power flow measurements missing for one bus). The simulation is performed for both a single branch and a larger network consisting of four different busses. The theory developed in this section is then supposed to be used as a background when assessing the uncertainties of the SE that is caused by various parameter errors.

5.2.1 Sensitivity analysis for a single branch

In order to simplify the comparison of the results, a single branch will be examined for two levels of transferred active power. The measurement data along with the actual parameter values are presented in appendix A. The data is taken from a branch within the Swedish transmission grid and is thus exemplifying a probable scenario. A 10 % error for all the different line parameters is then introduced to the simulations. The following simulations are performed for both a high (0.5 p.u.) and a low (0.1 p.u.) level of transferred active power. The simulation will examine the following two events:

- **Full measurement redundancy with perfect measurements and a line parameter error**: A single parameter error is introduced to the system that is otherwise consisting of perfect measurement. The SE algorithm is performed on the system and the error between the true measurement values and the estimated measurement values are then calculated. This error represents thus the sensitivity of the model for different parameter errors.
- **Reduced measurement redundancy with perfect measurements and a line parameter error**: The same simulation as previously is performed, however, in this case with power flow measurements only in the sending end. The SE algorithm is then again performed on the system and the error between the true measurement values and the estimated measurement values are then recalculated.

5.2.2 Sensitivity analysis for a radial topology

The effect that parameter errors have on a larger network is more complex than in the case of a single branch. Not only may the power flow and voltages vary in the system, but there may also be different combinations of parameter errors that increase the error magnitude significantly. In general, the highest relative errors are found when the transferred power flow of one branch is small compared to the others branches. Since the errors caused by an erroneous parameter in general affect the absolute errors for all measurements in some extent, a small absolute error may result in a very large relative value. Since the relative errors will vary with each combination of different power flows and parameter errors, it would be mathematically unfeasible to test all combinations, and no fixed uncertainty value may be attributed to parameter errors. Instead, the following simulation strives to develop a method of evaluating and finding the largest uncertainty for each specific system.

The design of the analysed network is presented is shown in Figure 5. Furthermore, the different parameter values along with the perfect measurements and the rated loads for all buses are presented in Table 13 in appendix A. The following procedure is then performed:

- The true model of the system is defined and the true states of all buses are calculated by using a standard load flow program for the network. Two different load flow conditions are examined:
    1. **Case 1**: Low load on bus 6, high load on the remaining load buses
    2. **Case 2**: Low load on all load buses
- Parameter errors are then introduced for the different line sections, with one parameter error each at a time. The relative difference between the estimated values and the true measurement for each parameter error and power flow case is then saved in the tables found in appendix B.
- A worst-case error caused by parameter errors can then be found by using the theory of superposition and combining the errors found in step 2. In this manner, it is possible to find an approximate uncertainty value in the SE due to the worst combinations of parameter errors.

In addition, a simulation of how errors in the measurement infrastructure affect the output of the SE for different levels of power flow is also performed. If the magnitude of the SE errors varies differently for errors in the measurement infrastructure than for errors in line parameter values, methods of differentiating these errors may be developed.

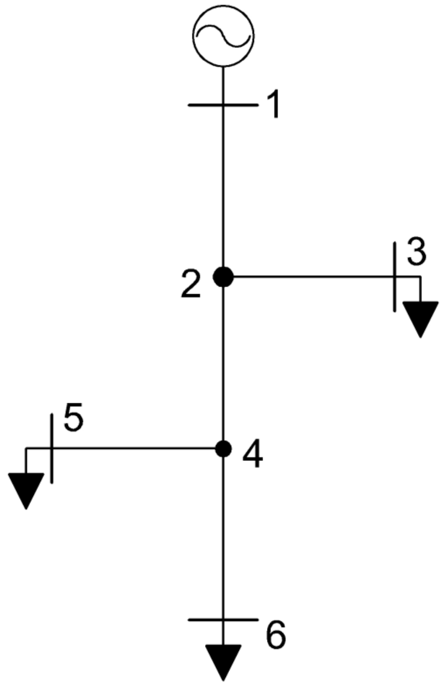

Figure 5. 4-bus network analysed used in the parameter sensitivity analysis for a radial topology

5.3 Simulation III: Theoretical parameter estimation

In order to evaluate and use the PE in a real-life environment, it is first required that a theoretical framework is established. Several previous studies have examined PE by generating data and adding noise to the “measurements” and then introducing a parameter error. However, if there is no linear error present, the parameter estimation will always converge very close to the actual parameter value, and the results are thus not specifically interesting.

To prevent this, a linear error to one of the measurements should be included. At that point, if the PE algorithm is still able to estimate and reach the correct value of the erroneous parameter, the estimation can be assumed to be accurate. In order to simulate this event, the following properties of the simulation are applied:

- **Single branch with power and voltage measurements**: Measurement data from one end of the branch is acquired from Svk during 96 hours and the data in the other end is calculated by using two-port equations. Perfect measurement data is thus generated.

- **Addition of measurement noise**: Measurement noise is added to the calculated "perfect "measurements. The noise magnitude is chosen to 0.5 % of the measured value.
- **Adding a linear measurement error and a parameter error**: The challenge for the PE algorithm is if it is possible to both have a relatively large measurement error and still being able to detect and estimate a better parameter value.

Analysing the effect of varying the initial parameter error is not of high importance in this case as the parameter estimation, if converging, should reach the same end value irrespectively of the initial value. However, the magnitude of the linear measurement error should be varied as this in a high extent will affect the PE. Furthermore, the type of measurement error should also be analysed. Thus, several error magnitudes and measurement error types will be examined.

In this simulation, the variance of all measurements is set to an equal value, resulting in a fully symmetrical weighting matrix. The initial variance of the erroneous parameter is set to a value of 100 times higher than the value of the measurements. This is to ensure that the estimation of the parameter is fast enough to converge. As the Kalman filtering is continuously updating the parameter variance, this value is quickly tuned to a smaller value. The estimation is performed for each parameter in the normal SE algorithm; the line conductance, line susceptance, and the shunt susceptance. The shunt conductance is in this case ignored as it is generally considered to be negligible. The results are presented in section 6.3 and then further discussed in section 7.3. An example of the MATLAB code used for the estimation of line susceptance is presented in Appendix C.

5.3.1 Accuracy improvement by using parameter estimation

In order to evaluate the accuracy improvement by using PE, a similar simulation as in section 5.2 is performed. However, in this case, the error caused by the line susceptance is only examined since an error in this parameter probably has the highest impact on the SE. The following case will thus be examined:

- **Full redundancy with measurement and line susceptance error**: A single voltage measurement error of 0.1% from the sending end is applied to the system that is otherwise consisting of perfect measurements with added noise. The SE algorithm is performed on the system, with and without the parameter estimation included. The average error between the "true" measurement values and the estimated measurement values are then calculated for both the scenario with PE and the scenario without the inclusion of PE.

In order for the PE to have time to converge and estimate a final value for the line susceptance, only the mean error for the last 24 hours of measurement data is chosen. Furthermore, the voltage measurement error is intentionally chosen to a somewhat small value. A too large measurement error would otherwise result that the effect of the parameter error in the accuracy of the SE would be negligible in comparison to the error from the measurement. The goal of this simulation is thus to examine how much the SE may be enhanced by implementing the PE algorithm. Furthermore, the overall uncertainties of the SE due to parameter errors may in this manner be examined.

5.4 Simulation IV: Alternative method of line resistance estimation

In this case, the alternative method for estimating line resistance that was presented in section 4.4 is analysed. The same branch parameter values and measurement values as in simulation 5.3 are used for this simulation. Following, perfect data is generated as a reference, and then noise and a linear error is implemented on one of the measurements. The relative line losses are then calculated from the measurements according to

$$|P_{f\%}| = \frac{P_{12m} + P_{21m}}{(S_{12m} - S_{21m})/2} = \frac{P_f}{S_{trans\_m}} \tag{5.1}$$

where P_{12m}, P_{21m} : measured active power from the sending and receiving end

S_{12m}, S_{21m} : measured apparent power from the sending and receiving end

S_{trans_m} : average transferred apparent power

In (5.1) and for the upcoming simulations, the direction of the power flow is defined by the subscript of the symbol. Thus, S_{12m} represents in this case the measured apparent power from the first node (1) to the second node (2). Equation (5.1) is then multiplied with the average voltage level as in (4.16) and the slope of the now plotted curve is then estimated and will be approximately equal to the line resistance. The slope of the plotted curve is found by using a Theil-Sen estimator (TSE). It is a more robust method for linear regression that uses the median slope among all lines through the pairs of the sample points. In this manner, the significance of outliers from the measurements is reduced. For more information regarding the TSE, the reader is referred to [19]. By using this method, the calculated slope of the curve will represent the estimated resistance of the line.

By examining (5.1), it is possible to deduct that a linear error in the active and reactive power measurements will affect the result by both shifting the plotted relative losses vertically and affecting the slope of the plotted line. Similarly, a linear error in the voltage measurement will instead mainly affect the slope of the curve. The accuracy of this approximation is then evaluated for several magnitudes of measurement errors in both the active and reactive power measurements as well as for errors in the voltage measurements. The results of the estimation are presented in section 6.4.

6 Results

In the following section the results from the performed simulations in section 5.1-5.4 are presented. The results are presented in the same order as the simulations and the results are then summarised and further discussed in the following section.

6.1 Model sensitivity analysis

The results of the analysis between the single-phased model, and the proposed three-phase model are presented in this section. Table 2 presents the voltage and current difference for each phase for different levels of asymmetry. The summated average difference for all phases is also computed. From the table it is possible to deduce that already at low levels of asymmetry, the results between the single-phase and the three-phase model differs relatively much if each phase is considered. The voltage varies up to 0.82 percent per phase at higher levels of asymmetry according to the table. The difference between the two models is, not surprisingly, decreasing significantly with the magnitude of the asymmetry, and at the lower value of asymmetry the difference is somewhat negligible.

Table 2. Difference in percentage between the single-phase model and the proposed three-phase model

	High asymmetry		**Medium asymmetry**		**Low asymmetry**	
	Voltage [%]	**Current [%]**	**Voltage [%]**	**Current [%]**	**Voltage [%]**	**Current [%]**
Phase A	0.819	-0.465	0.409	-0.233	0.205	-0.117
Phase B	-0.086	0.040	-0.044	0.020	-0.022	0.010
Phase C	-0.725	0.431	-0.363	0.215	-0.182	0.107
Summated avg. difference for all phases	0.0025	0.0019	0.0006	0.0005	0.0002	0.0001

However, by summating and calculating the average of the phase magnitudes, the difference for all levels of asymmetry is found to be very small. For the highest level of asymmetry, the average voltage magnitude differs only with a level of 0.0025 % between the equivalent single-phase model and the proposed three-phase model. Hence, it is possible to assume that from calculations of average power flow and average voltage magnitudes that the single phased model could be considered sufficient.

In Figure 6, the simulated line losses for each phase is plotted with respect to the total transferred active power for the three-phase model in the case of a highly asymmetric line. As can be found in the figure, the active power losses vary significantly for each phase due to the unbalanced grid. The difference is especially high during very light loads and during high loads, as the mutual impact of the other adjacent lines differs significantly between these states. However, if the total line losses of the three-phase model are calculated, the total losses of this model conforms almost perfectly with the total line losses for the equivalent single-phase model. Thus, yet again, if the total average value is of interest, the single-phase model is found to be sufficiently accurate.

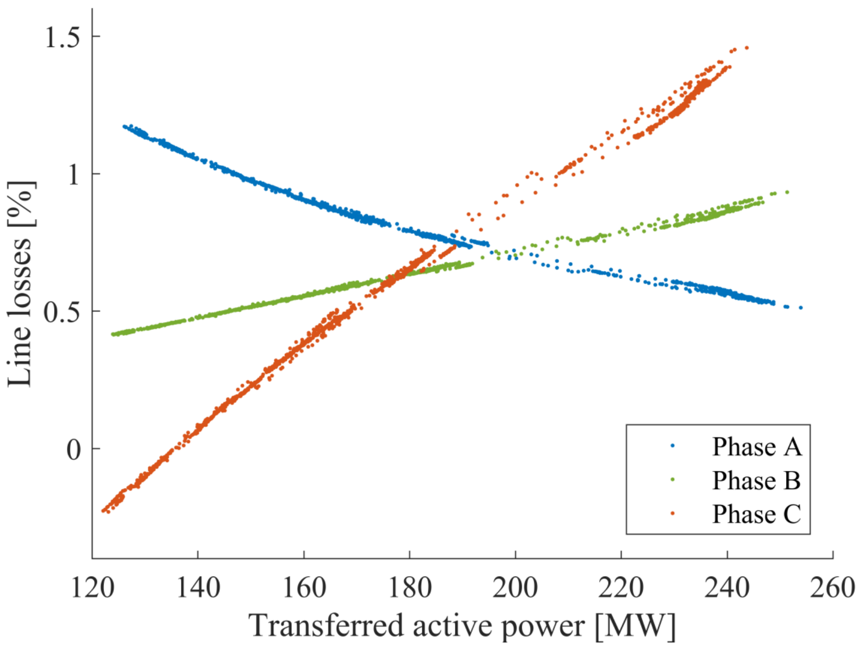

Figure 6. Simulated line losses for each phase plotted with respect to total transferred active power for a single transmission line modelled with the developed three-phase model

6.2 Parameter error sensitivity analysis

The results from the simulations in section 5.2 are presented here. The results are first presented for the sensitivity analysis for the single branch followed by the results for the larger network, and the results are then further discussed in section 7.2.

6.2.1 Sensitivity analysis for a single branch

In Table 3, the relative error between the true and the estimated values in the case of perfect measurements and a 10 % parameter error is presented. The impact on the estimated values caused by errors in the line susceptance (b_{12}), line conductance (g_{12}), and shunt susceptance is examined (bs_1). According to the results, even a 10 % parameter error is generally affecting the output of the SE marginally for most of the measurements. The relative errors of the reactive power are found to be the largest, which may be explained by the fact that the transmitted reactive power is very small in comparison to the absolute error. Furthermore, the largest effect on the output of the SE is found to be originating from errors in line susceptance, where for example a 10 % error would result in 0.114 % error in the P_{21}-measurement.

Table 3. Relative error between the true and estimated values. For perfect measurements and full measurement redundancy and a line parameter error of 10 %

	Relative estimation error for measurement					
	$\boldsymbol{P_{12}}$ **[%]**	$\boldsymbol{P_{21}}$ **[%]**	$\boldsymbol{Q_{12}}$ **[%]**	$\boldsymbol{Q_{21}}$ **[%]**	$\boldsymbol{V_1}$ **[%]**	$\boldsymbol{V_2}$ **[%]**
Estimation error for high amount of transferred power						
Error in $\boldsymbol{b_{12}}$	0.024	-0.114	-3.388	4.663	0.039	0.014
Error in $\boldsymbol{g_{12}}$	-0.029	0.030	-0.063	-0.012	-0.029	0.030
Error in $\boldsymbol{bs_1}$	-0.053	-0.053	-4.498	6.147	0.032	0.031
Estimation error for low amount of transferred power						
Error in $\boldsymbol{b_{12}}$	0.024	-0.021	-0.195	0.1860	-0.061	0.063
Error in $\boldsymbol{g_{12}}$	-0.009	0.010	-0.006	-0.009	-0.006	0.006
Error in $\boldsymbol{bs_1}$	-0.054	-0.053	-2.879	6.157	0.020	0.018

The difference between a high and a low amount of transferred power is found to have the largest effect for errors in the line susceptance and the line conductance. For the lower amount of transferred power, the errors are reduced significantly for both of the measurements. However, the estimation error caused by errors in the shunt susceptance is found to be relatively the same for both power levels.

In Table 4, the results when the power flow measurements of P_{21} and Q_{21} are missing are presented. The error of estimating the unmeasured values are increasing significantly for errors in both the line susceptance and the line conductance. The very high erroneous value for the reactive power of Q_{21} is yet again a result from the fact that the transferred reactive power is rather small in this case, resulting in large relative errors. Another result to notice is that the errors for the measured values are found to be more accurate than in the case of full redundancy. The difference between the high and the low amount of transferred power is yet again proved to have the same effect. The estimation errors are reduced with the power level for errors in line susceptance and line conductance, but may be considered almost constant in the case of errors in the shunt susceptance.

Table 4. Relative error between true and estimated values for perfect measurements with reduced measurement redundancy and a line parameter error of 10 %

	Relative estimation error for measurement					
	$\boldsymbol{P_{12}}$ **[%]**	$\boldsymbol{P_{21}}$ **[%]**	$\boldsymbol{Q_{12}}$ **[%]**	$\boldsymbol{Q_{21}}$ **[%]**	$\boldsymbol{V_1}$ **[%]**	$\boldsymbol{V_2}$ **[%]**
Estimation error for high amount of transferred power						
Error in $\boldsymbol{b_{12}}$	~ 0	-0.139	-0.029	9.530	-0.011	0.011
Error in $\boldsymbol{g_{12}}$	~ 0	0.059	-0.072	0.025	-0.029	0.030
Error in $\boldsymbol{bs_1}$	~ 0	-0.001	-0.066	12.677	-0.027	0.027
Estimation error for low amount of transferred power						
Error in $\boldsymbol{b_{12}}$	~ 0	-0.039	-0.110	0.380	-0.062	0.063
Error in $\boldsymbol{g_{12}}$	~ 0	0.020	-0.010	-0.017	-0.006	0.006
Error in $\boldsymbol{bs_1}$	~ 0	-0.004	-0.042	12.618	-0.027	0.027

6.2.2 Sensitivity analysis for a radial topology

In the following section the results from the sensitivity analysis for the 4-bus network is presented. The results concerning the sensitivity analysis for this simulation are naturally more complex than the sensitivity analysis for the single branch. The full tables of all the combinations of parameter errors for the two different power levels are presented in their entity in Table 15 and Table 16 in appendix B. In this section the main conclusions that may be drawn from these simulations are presented.

Table 5 presents the effect that a 10 % parameter error in branch 1-2 from the grid configuration in Figure 5 has on the output of the SE for two different levels of power flow. The impact on the estimated values caused by errors in the line susceptance (b_{12}), line conductance (g_{12}), and shunt susceptance is examined (bs_1). According to Table 5, the estimation errors are in general higher for the case with 20 % of rated power in bus 6 and full rated power of the other buses, than for the case with 20 % rated power in all buses. The difference is especially significant for errors in the active and reactive power measurement, where for example the error in the estimation of P_{64} is reduced from an error value of -3.086 % to 1.202 for an error in the line susceptance. The error in the voltage estimation is however found to be relatively independent on the power flow levels.

Another aspect to notice is that the highest relative errors in power flow occur for branches with relatively low levels of measured power. In the case with 20 % of rated power in bus 6 and full rated power of the other buses, the error for the active power estimations in bus 6 is significantly higher for the bus with the reduced load, compared to the buses with 100 % load. However, it is yet again found that the estimation errors in the voltages are more or less independent on the current load flow. Furthermore, the highest errors are in general found to be correlating with errors in the line susceptance; an outcome that is consistent with the results from the single branch analysis. An analysis of parameter errors on the other branches shows that the branches with high impedance values - in general longer or poorly dimensioned lines - are most sensitive to parameter errors. For example, branch 1-2 is the branch with the highest impedance and a relative parameter error for this branch results in larger estimation errors than for errors in branches with lower impedance.

Table 5. Relative estimation errors for different parameter errors and load flows for a 4-bus network

	Parameter errors of 10 %					
	20 % of rated power in bus 6 100 % of rated power in remaining buses			**20 % of rated power in bus 6 20 % of rated power in remaining buses**		
Est. error in [%]	g_{12}	b_{12}	bs_1	g_{12}	b_{12}	bs_1
V_1	0.094	-0.094	-0.021	0.026	-0.138	0.026
V_3	-0.042	0.016	-0.001	-0.011	0.057	-0.011
V_5	-0.031	0.039	0.011	-0.008	0.046	-0.008
V_6	-0.022	0.057	0.019	-0.006	0.036	-0.006
P_{12}	0.028	-0.220	-0.105	-0.037	0.252	-0.037
P_{32}	-0.018	0.060	0.029	0.022	-0.178	0.023
P_{54}	-0.117	0.264	0.121	0.046	-0.520	0.046
P_{64}	-1.436	-3.086	-1.474	-0.353	1.202	-0.353
Q_{12}	-20.842	171.790	29.065	0.555	-2.925	0.555
Q_{32}	3.053	22.812	8.819	0.953	-2.310	0.953
Q_{54}	5.122	17.940	7.599	1.469	-4.985	1.469
Q_{64}	5.916	10.954	5.272	1.642	-6.291	1.642

The highest estimation error caused by parameter errors may be found by combining the different combinations of parameter errors that will contribute to the largest estimation error. In Table 6, the largest errors for the different combinations of parameter errors are presented for a small selection of measurements to exemplify the effect. The load flow conditions are chosen to the case with 20 % of rated power in bus 6 and full rated power of the other buses.

According to the table, the SE error may increase significantly if the parameter errors are combined in an undesirable way. The power flow estimations are in general found to be more sensitive for combinations of parameter errors than the voltage estimations. Important to note for this simulation, is that it is *highly* unlikely that all parameter errors contribute to a worst-case scenario. Furthermore, the parameter error level of 10 % that is used in the simulation is in most cases greatly exaggerated and the total errors may in general be significantly less. However, the general effect that these combinations of parameter errors produce is still important.

Table 6. Largest state estimation error due to worst case scenario of parameter errors

Measurement	Largest estimation error [%]
V1	0.2274
V6	0.1409
P1	0.4585
P6	8.1125

An analysis of how measurement errors affect the output of the SE was also performed. The full results from the simulation are not presented in this section due to the size and number of tables, but the main findings will be presented. The full tables for the two power flow levels are found in Table 17 and Table 18 in appendix B. A linear error in the voltage or the power flow measurements is found to result in relatively constant SE error, regardless of the power flow levels in the system. This can be compared with the case of parameter errors that was found to result in large differences in SE error magnitudes for different power flow levels. Thus, if the power levels are varying and the size of the residuals are varying as a consequence, this may be assumed to be a result mainly due to parameter errors.

6.3 Theoretical parameter estimation

The results from the simulations presented in section 5.3 are presented here. The theoretical PE simulation is performed by using the properties of a single branch as was previously explained. The initial value of the erroneous parameter is for all simulations set to a value of 0.9 times the actual parameter value. This parameter error represents thus an error that may be present in a regular transmission line.

Single measurement errors are added to the system together with the parameter estimation in order to analyse what measurement error that has the highest effect on the accuracy of the PE. The percentage change between the final estimated parameter and the true parameter value is then entered as a result into Table 7 - Table 9. The results for each parameter error are presented separately as these results differ significantly.

6.3.1 Estimation of line susceptance

In the following section, the accuracy of the PE in the case of a line susceptance error is presented. The full results with the different combinations of measurement errors and error magnitudes may be found in Table 7. According to the results, the estimation of line susceptance is highly accurate for measurement errors in both active and reactive power. Even for measurement errors in the range of 2 % in the power flow measurements P_{12} and Q_{12} results only in estimation errors of up to around 3 %. However, the accuracy of the PE is found to be more sensitive for errors in the voltage measurement devices. Errors above 1 % in the voltage measurement results in a parameter error that is equal, or even higher, than the initial erroneous value. For errors in both the voltage and the apparent power measurements, the PE errors are found to be in about the same range or less than for errors solely in the voltage measurement.

Table 7. Differences between estimated and true line susceptance value for varying magnitudes of different measurement errors

	Linear measurement error in			
	$\boldsymbol{P_{12}}$	$\boldsymbol{Q_{12}}$	$\boldsymbol{V_1}$	$\boldsymbol{V_1 + S_{12}}$
Measurement error [%]	**Est. $\boldsymbol{b_{12}}$ error [%]**	**Est. $\boldsymbol{b_{12}}$ error [%]**	**Est. $\boldsymbol{b_{12}}$ error [%]**	**Est. $\boldsymbol{b_{12}}$ error [%]**
0.1	-0.17	-0.53	0.98	0.92
0.5	0.10	-0.92	4.85	4.39
1	0.58	-1.91	9.20	8.35
2	2.04	-3.32	16.99	15.32
5	5.29	-7.72	51.86	28.42

In Figure 7, the estimation of the line susceptance, along with the true parameter value, is illustrated in the case of a 0.5 % linear error in the voltage measurement for V_1. According to the figure, the estimation of the line susceptance quickly approaches the true parameter value but settles at a value differing 4.85 % from the true value. The reason for the irregular curve is that the added random noise of all measurements distorts the estimation. However, the Kalman filtering and the iterative process of the PE algorithm filters over time the added noise and converges to a final value.

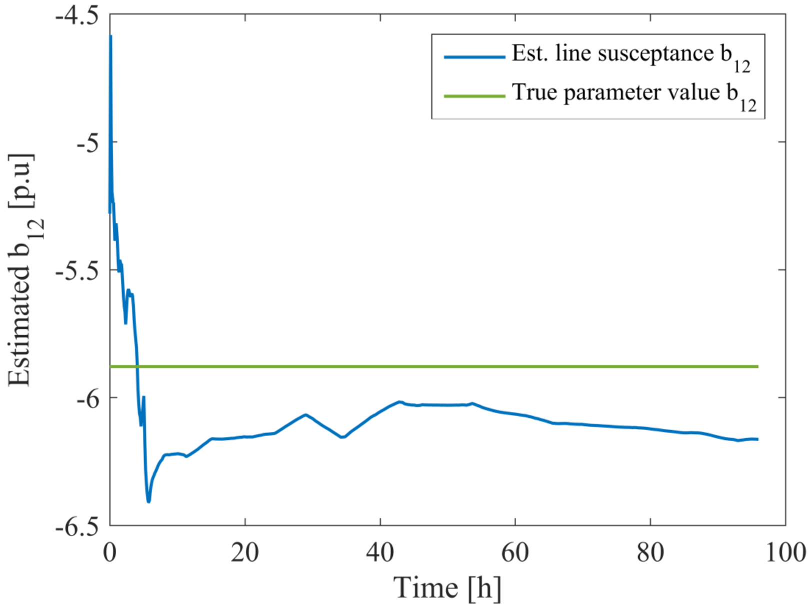

Figure 7. Estimated line susceptance and true parameter value for a 0.5 % error in the voltage measurement in the sending end of the line

In Figure 8 the estimated line susceptance is shown along with the true parameter value when there is a 0.5 % linear error in the active power measurement in the sending end of the line. In this case, the PE is highly accurate in estimating the line susceptance value and quickly settles at a value differing only 0.1 % from the actual parameter value.

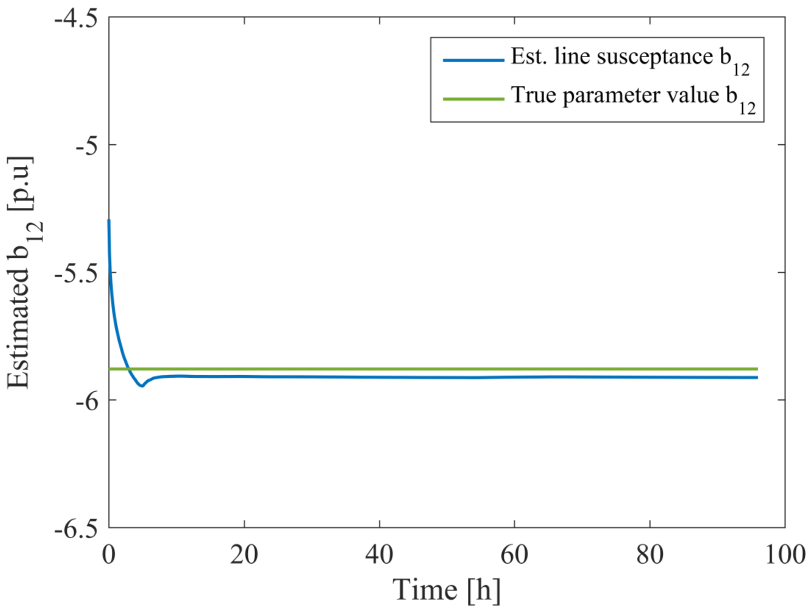

Figure 8. Estimated line susceptance and true parameter value for a 0.5 % error in the active power measurement in the sending end of the line

6.3.2 Estimation of line conductance

The accuracy of the PE in the case of a line conductance error is examined in the following section. The full results with the different combinations of measurement errors and error magnitudes may be found in Table 8. According to the table, the estimation of the line conductance is significantly more sensitive to errors in the voltage and active power measurements than for the case of the estimation of the line conductance. Even a 0.1 % error in the voltage measurement results in significant errors in the PE of the line conductance. For errors in both the voltage and the apparent power measurements, the PE errors are found to be in about the same range as for errors solely in the voltage measurement. Moreover, errors in the active power measurement results in large PE errors already at measurement errors of the magnitude of 0.5 %. At higher levels of measurement errors the PE estimates the line conductance to physically infeasible negative values, denoted in the table as '*Not-a-Number*' (NaN).

The estimation is found to be more or less insensitive with respect to errors in the reactive power measurements. Reactive power measurement errors with a magnitude of up to 2 % still results in accurate line conductance estimations. For lower levels of measurement errors the PE is found to be almost fully accurate.

Table 8. Differences between estimated and true line conductance value for varying magnitudes of different measurement errors

	Linear measurement error in			
	$\boldsymbol{P_{12}}$	$\boldsymbol{Q_{12}}$	$\boldsymbol{V_1}$	$\boldsymbol{V_1 + S_{12}}$
Measurement error [%]	**Est. $\boldsymbol{g_{12}}$ error [%]**	**Est. $\boldsymbol{g_{12}}$ error [%]**	**Est. $\boldsymbol{g_{12}}$ error [%]**	**Est. $\boldsymbol{g_{12}}$ error [%]**
0.1	-2.46	0.39	-24.25	-26.34
0.5	-13.58	-0.22	NaN	NaN
1	-26.74	-0.65	NaN	NaN
2	-53.25	-2.51	NaN	NaN
5	NaN	-5.78	NaN	NaN

In Figure 9 the estimated line conductance is instead illustrated along with the true parameter value when there is a 0.5 % linear error in the voltage measurement in the sending end of the line. As can be concluded by examining the figure, the PE algorithm is unfeasible to use for estimation of the line conductance when errors in the voltage measurement devices are present. The estimation of the parameter results in a negative value, which of course is physically unfeasible.

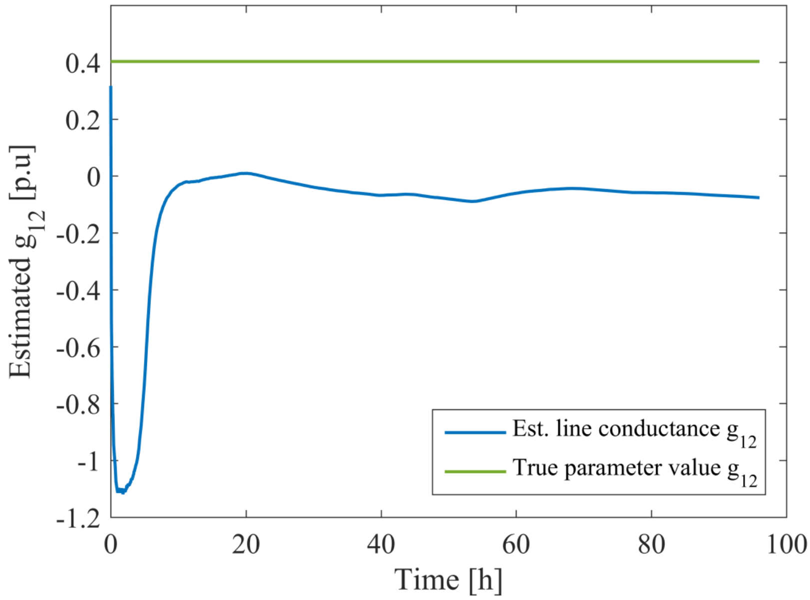

Figure 9. Estimated line conductance and true parameter value for a 0.5 % error in the voltage measurement in the sending end of the line

In Figure 10 the estimated line conductance is illustrated along with the true parameter value when there is a 0.5 % linear error in the active power measurement in the sending end of the line. The resulting end value of the estimation is differing -13.58 % from the actual parameter value, thus even worse than the initial value of 10 %. The irregular curve of the estimation is yet again a result due to the added measurement noise. As can be found in the figure, the estimation algorithm is however quickly tuned close to the final value after a few estimations.

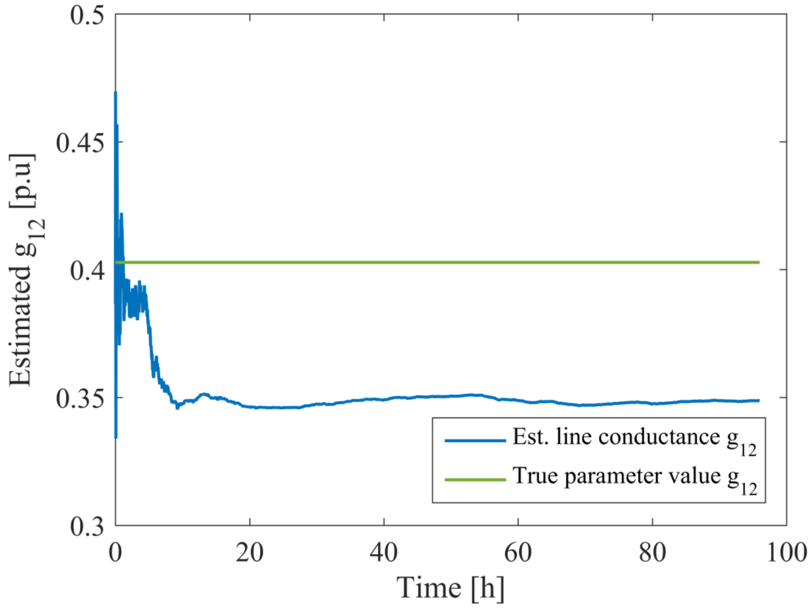

Figure 10. Estimated line conductance and true parameter value for a 0.5 % error in the active power measurement in the sending end of the line

6.3.3 Estimation of shunt susceptance

The accuracy of the PE in the case of a shunt susceptance error is examined in the following section. The full results with the different combinations of measurement errors and error magnitudes may be found in Table 9. According to the table, the estimation of the shunt susceptance is highly sensitive to errors in the voltage measurements. An error of the magnitude of 0.1 % for the voltage measurement, results in significant errors in the PE. For voltage measurements errors with a magnitude of 1 %, the estimation results in unfeasible negative values.

The estimation of the shunt susceptance is on the other hand found to be somewhat insensitive to measurement errors in the power measurements. Errors in the active power measurement results in only very marginal errors on the PE and only higher levels of error in the reactive power measurement distorts the results of the PE.

Table 9. Differences between estimated and true shunt susceptance value for varying magnitudes of different measurement errors

	Linear measurement error in			
	P_{12}	Q_{12}	V_1	$V_1 + S_{12}$
Measurement error [%]	**Est. bs_1 error [%]**	**Est. bs_1 error [%]**	**Est. bs_1 error [%]**	**Est. bs_1 error [%]**
0.1	0.12	0.12	-18.61	-18.07
0.5	0.15	0.63	-72.34	-99.18
1	0.14	0.81	NaN	NaN
2	0.16	-2.52	NaN	NaN
5	0.20	-6.62	NaN	NaN

In Figure 11 the estimated shunt susceptance is illustrated along with the true parameter value when there is a 0.5 % linear error in the voltage measurement in the sending end of the line. The estimation is found to be highly misleading with an error of 72.34 %. Due to the fact that the shunt susceptance is significantly smaller in magnitude than for example the line susceptance, the estimation of the parameter is somewhat noisy.

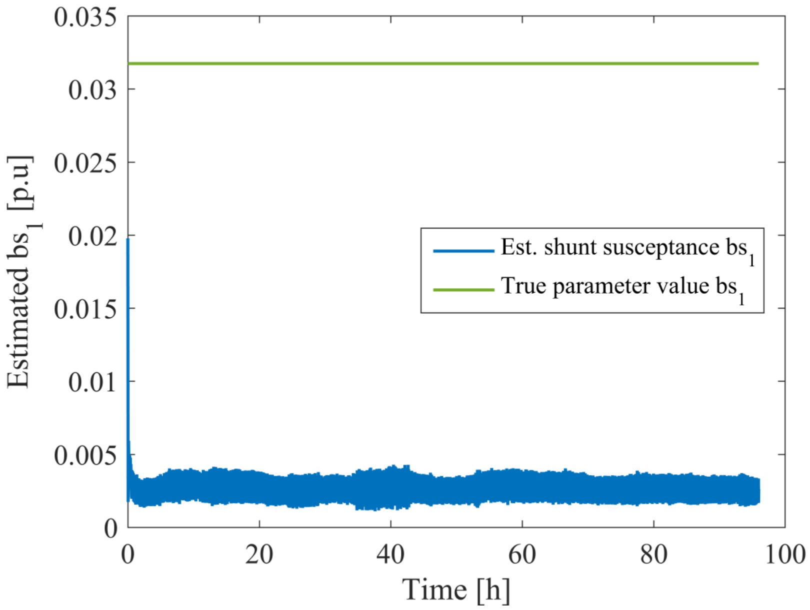

Figure 11. Estimated shunt conductance and true parameter value for a 0.5 % error in the voltage measurement in the sending end of the line

In Figure 12 the estimated shunt susceptance is illustrated along with the true parameter value when there is a 0.5 % linear error in the active power measurement in the sending end of the line. In this case, the estimation is found to be very accurate and is quickly converging with the actual value. The noise of the parameter estimation is however still present.

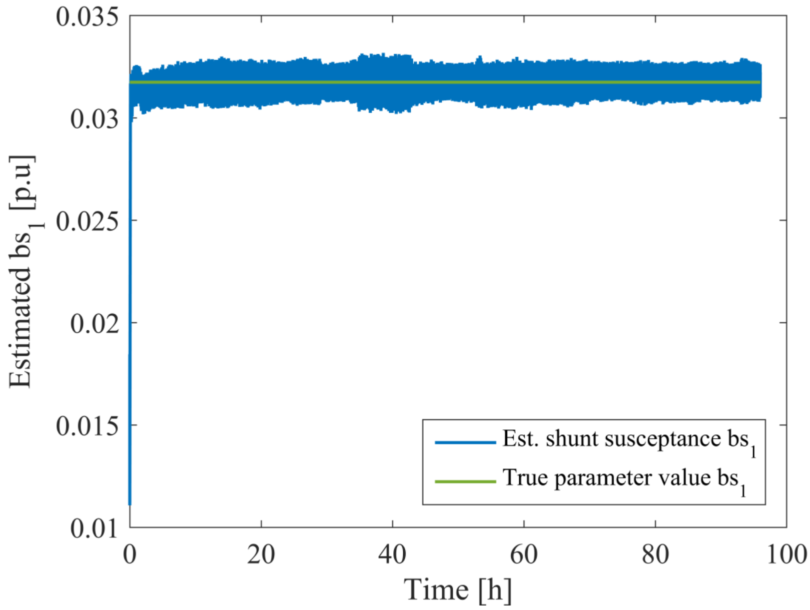

Figure 12. Estimated shunt conductance and true parameter value for a 0.5 % error in the active power measurement in the sending end of the line

6.3.4 Accuracy improvement by using parameter estimation

In Table 10, the results are presented for the simulation when a 0.1 % measurement error is introduced in the voltage measurement for V_1, and a 10 % error in the line susceptance (b_{12}). The accuracy of the estimation of the line susceptance for this measurement error was presented in the previous section. According to the table, the mean SE error is significantly reduced for all measurements when the PE algorithm is introduced. The estimated voltage error for V_1 is for example reduced from 0.0741 % to 0.0481 % when PE is implemented. Similarly, the estimated active power flow error for P_{12} is reduced from 0.0202 % to 0.0033 %. The most significant change is the one for the reactive power measurement in the receiving end of the branch. This large error is however mostly due to the fact that the sampled reactive power transmitted on the line is very small, thus resulting in very large relative errors.

Table 10. Mean error between the true and estimated values for a SE with and without PE implemented. Measurement error of 0.1 % in V_1 and line susceptance (b_{12}) error of 10 % is introduced in the simulation

Measurement type	P_{12}	P_{21}	Q_{12}	Q_{21}	V_1	V_2
Avg. error with PE [%]	0.0033	0.0016	0.2240	2.3110	0.0481	0.04826
Avg. error without PE [%]	0.0202	0.0489	2.6810	45.230	0.0741	0.0632

6.4 Alternative method of line resistance estimation

In the following section the results from the alternative method of line resistance estimation are presented. The full results with the different combinations of measurement errors and magnitudes may be found in Table 11. In this case, the measurement errors for the transferred power are lumped for both the active and reactive power. According to the table, the estimation is found to be significantly less sensitive to measurement errors in the voltage measurements. Even a voltage error of 5 % results only in a resistance estimation error of 4.51 %. The estimation was however found to be more sensitive to measurement errors in the power flow measurements and errors above 0.5 % resulted in relatively bad estimations. For measurement errors in both the apparent power and the voltage, the accuracy was found to be significantly worse. In general however, the alternative method presented better estimations for all levels of measurement errors than the ordinary estimation method.

Table 11. Differences between estimated and true line resistance value for varying magnitudes of different measurement errors for the alternative method of estimating line resistance

	Measurement error in		
	S_{12}	V_1	$V_1 + S_{12}$
Measurement error [%]	**Est. g_{12} error [%]**	**Est. g_{12} error [%]**	**Est. g_{12} error [%]**
0.1	-2.09	-1.98	-4.36
0.5	-5.63	-1.98	-6.83
1	-7.86	-1.98	-9.53
2	-14.79	-2.63	-16.12
5	-29.42	-4.51	-42.01

In Figure 13 the relative line losses, multiplied with the actual voltage level, are plotted with respect to transferred apparent power for the case of a 0.5 % error in the voltage measurement in the sending end. The green circles are illustrating the true points in the perfect system and the blue points are the measured data values, with noise and a linear error present. The teal line is the Theil-Sen regression line for the measured values, where the slope of the line is representing the estimated resistance. The red line is a regression line illustrating the slope for a 10 % error in the resistance. The figure clearly shows that the regression line, giving the estimated value of the resistance, correlates very closely to the slope of the actual true data points. The estimation is thus in this case highly accurate.

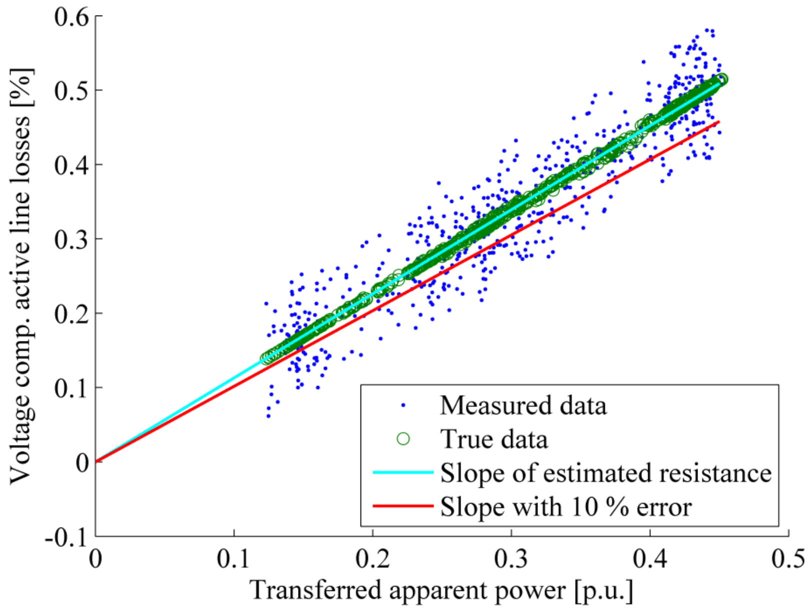

Figure 13. Voltage compensated active line losses plotted with respect to transferred apparent power for measured data and true data. The estimated slope of the measured data, which is the estimated resistance, as well as a reference slope based on a resistance with a 10 % error is also presented

In Figure 14 the same relative line losses, multiplied with the actual voltage level, are plotted with respect to transferred apparent power but in this case for an error of 0.5 % in the power flow measurement in the sending end. The green circles are yet again illustrating the true points in the perfect system and the blue points are the measured data values, with noise and the linear error present. In this simulation, there is a linear shift of the actual true values and the measured data due to the error in the power flow measurement in the sending end. However, even though the data is shifted, it is possible to estimate the resistance since the slope of the measured data points should not be affected as much. According to figure, the estimated slope is fairly close to the slope of the true values, and the error is estimated to -5.63 %. This error thus represents the error in the resistance estimation. The accuracy of this estimation is, despite a fairly large error, still more accurate than the ordinary PE algorithm.

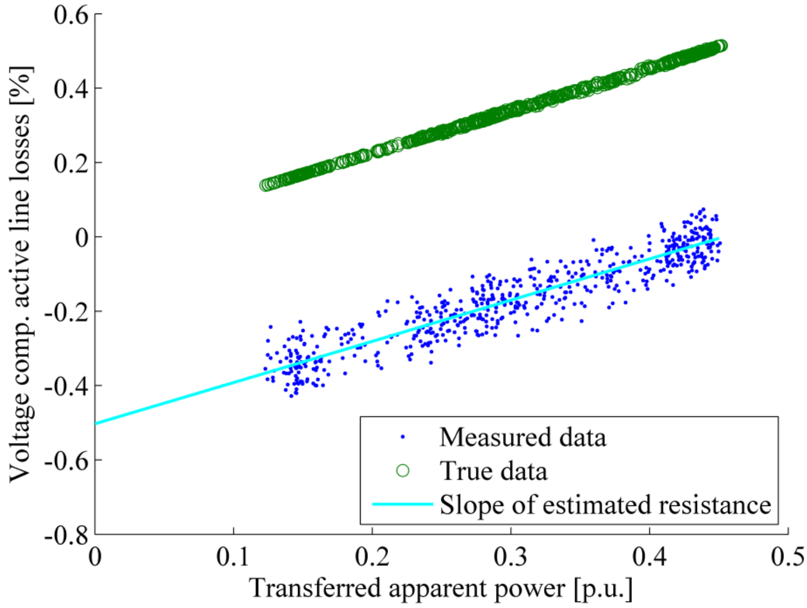

Figure 14. Voltage compensated active line losses plotted with respect to transferred apparent power for both measured data and true data together with estimated resistance line

The vertically shifted curve also provides information that there is a probable linear error in either one or both of the power flow measurements. Thus, by evaluating the slope of the relative line loss curve it is also possible to deduct if there are measurement errors are present in the system. An inspection and calibration of the measurement devices could thus be performed if such errors are found. It is in this case possible to estimate the size of the linear error by examining the value of the estimated resistance line at the zero level of the transferred apparent power. In Figure 14 the value at no transferred power is about -0.5 % which is consistent with the applied error in the power flow measurement. However, the problem remains in establishing in what end of the branch the linear error is located.

The resistance estimation could however be improved by taking this information into account. If either one of the power flow measurements are compensated with the same level as the estimated linear error, the estimation of the line resistance will be significantly enhanced. This is true even if it is the non-erroneous measurement that is being compensated. The feasibility of using this method is further discussed in section 7.4.

7 Discussion

An accurate and precise SE is essential for the grid planning and the operation of the power system. Other applications, such as detection of malfunctioning measurement devices, may be developed if the accuracy of the SE is sufficiently high. In the following section the results from 6.1-6.4 are discussed and analysed. Each simulation is analysed separately, followed by a comprehensive discussion of the general results. Moreover, the results are discussed with respect to if and how they may be used practically for increasing the accuracy of the SE model.

7.1 Model sensitivity analysis

The results found in section 6.1 demonstrate the impact of using the equivalent single-phase model in the case of an asymmetric line. The phase values were found to be varying significantly for all levels of asymmetry when comparing the single-phase model with the more detailed three-phase model. In the case with the highest asymmetry, the phase voltages varied with magnitudes up to 0.8 %, a value that by itself exceeds the measurement requirements of ±0.5 % from SWEDAC. Furthermore, the line losses of the asymmetric line are also found to be significantly varying from the single-phase model as is illustrated in Figure 6. Lower levels of asymmetry results in, not surprisingly, lower levels of phase differences.

However, the impact of an asymmetric line on the outcome of the SE is perhaps not as significant as first might be the impression. For the general SE model, the *average* values for the phase voltages, the active power, and reactive power are used as an input. By computing these averaged phase values for the three-phase model, it is found that the resulting average values are differing only marginally from the calculated equivalent single-phase values. The averaged line losses for the three phases are also found to be almost perfectly equal to the line losses for the single-phase model. Thus, when averaged phase values are used for the analysis in the SE model, it would be sufficient to use the equivalent single-phase model and still keep a high accuracy of the estimation, even in cases of high asymmetry. One of the main goals of the SE is to estimate the total power flows of the power system, and in this aspect the asymmetry affects only the outcome of the estimation negligibly.

7.2 Parameter error sensitivity analysis

The results found in section 6.2 are discussed and analysed in this section. The results for the single branch and for the 4-bus network are discussed separately as the method differed significantly between the two simulations.

7.2.1 Sensitivity analysis for a single branch

In section 6.2.1, several simulations regarding the accuracy of the SE when parameter errors are present were performed for the single branch. In general it was found that parameter errors do not affect the output of the estimations in such a high degree as first may be predicted. In the case of full redundancy, with power flow and voltage measurements for both buses, the estimation errors were found to be relatively small for all measurements. The reason for the higher relative errors for the reactive power flow is the fact that the transferred reactive power is so small in this case, so that even a small absolute error results in a large relative error.

The full redundancy is the key to explain the relatively small effect that parameter errors have on the result. Since the erroneous parameters only affects the calculations of the system measurement functions, the calculations of the power flow measurement functions will be affected initially. However, since the calculated values of the power flows will be erroneous due to the parameter errors, the estimator will try to alter the voltage values slightly to decrease these errors. When the sum of all the squared residuals is as small as possible the estimator has converged. Since all values are measured it will be impossible to alter one value without increasing the residual of another and the estimator will thus only adjust the estimated values slightly. The final result is that the error caused by the erroneous parameter is affecting all measurement functions by only a negligible degree.

In the case of reduced redundancy the effect of parameter errors have increased, yet is still not very significant. The estimation errors increased for both of the missing power flow measurements, but were found to be reduced for the remaining measurements. The larger relative error for the reactive power may yet again be explained by the low transferred reactive power of the line.

7.2.2 Sensitivity analysis for a radial topology

The sensitivity analysis for the 4-bus network resulted in several notable findings. Primarily, a non-desirable combination of parameter errors was found to significantly reduce the accuracy of the SE. The loss of accuracy was especially significant for the power flow measurements. However, it is necessary to remember that it is highly improbable that all parameter values in a network contribute to the highest error. Thus, the values found in Table 5 and Table 6 should be considered rather as example values in an illustrative sense. The magnitude of the parameter errors in the simulation are also chosen to a value of 10 %, which is in most cases also highly exaggerated. When assessing the errors in the SE caused by parameter errors, it is thus highly important to define both what magnitude of errors that may be expected, but also the probability that these errors contribute to a larger estimation error. The impact of parameter errors from computational errors should also be assessed. For example, if the distance between the transmission line conductors is poorly estimated, both the calculated inductance and the capacitance values will be affected. However, the impact by the computation error in the inductance may be countered by the error in the capacitance, and the total error in the SE may thus in fact be decreased.

The estimation errors due to parameter errors were also found to be significantly larger for the case with 20 % of rated power in bus 6 and full rated power for the remaining buses, than for the case with 20 % rated power for all buses. Different load flow situations will thus result in significantly different uncertainties due to parameter errors. This conclusion may prove highly useful when assessing the result of the SE in order to detect errors in the measurement infrastructure. In order to perform accurate error detection, the impact from parameter errors has to be minimized. By then choosing a load flow state with more evenly distributed power flow levels, the impact of parameter errors would be reduced. Furthermore, the estimation error for the bus with the lowest power flow was found to be significantly higher than for buses with comparatively high power flows. Detecting errors in the measurement infrastructure for those buses may thus prove to be troublesome. Since each network configuration and power flow state results in different sensitivities to parameter errors, a sensitivity analysis has to be performed for each case.

Errors in the line susceptance were yet again found to result in the highest levels of errors in the SE. Furthermore, relative errors in the branch with the highest impedance were found to have the highest impact on the outcome of the SE. The most important parameter to have correct data values for is thus the line susceptance in the branch with the highest impedance. Fortunately, the report found that the line susceptance can be estimated with reasonable accuracy in most instances. Since this is the parameter with the highest impact on the SE, it might be enough to estimate only this parameter.

7.3 Theoretical parameter estimation

The results from section 6.3 examine the possibilities and limits of using and implementing PE within the ordinary SE. The feasibility of estimating the line conductance, line susceptance, and shunt susceptance were examined in several cases of varying magnitudes of measurement errors. In the case of estimating the line susceptance, the estimation was found to be relatively resilient with respect to most measurement errors. Even high errors, above 2 %, in the active and reactive power measurement resulted in accurate estimations of that parameter. For the voltage measurements, errors up 0.5 % gave accurate results for the estimation. At measurement errors higher than these values, the accuracy of the PE started to decrease significantly. Thus, the PE for line susceptance was accurate for all the measurement errors within the stated measurement requirements of ±0.5 % by SWEDAC.

However, the estimation of the line conductance and the shunt susceptance was found to be highly inaccurate in the presence of measurement errors. Even marginally small voltage measurement errors resulted in heavily distorted PE of both the line conductance and the shunt susceptance. For example, errors in the active power measurements of a magnitude of 0.5 % and higher resulted in significant errors in the estimation of the line conductance. In contrast, the estimation of the shunt susceptance was found to be more or less independent on errors for these measurements. Instead, errors in the reactive power measurements were found to affect the estimation of the shunt susceptance in a higher degree, although first at higher levels of measurement errors.

The question that remains is why the line susceptance was found to be so much more accurately estimated than the other two line parameters. In addition, the estimation of most parameters was found to be more sensitive to errors in the voltage measurement devices, whilst at the same time almost non-dependent to errors in some the power flow measurements. The answer to why the estimation of line susceptance is more accurate than for example the estimation of the line conductance is that the line impedance of the examined line is consisting mainly of the line susceptance. The estimator attempts to tune the line parameter gradually to decrease the weighted residual between the measured and the estimated values as much as possible. Thus, if there is a single error in one of the active power flow measurements, the highest residual is found for this measurement. The estimator will then try to increase/decrease the estimated parameter to a value that reduces the total residuals for all measurements, as these are weighted by the weighting matrix. However, by tuning the parameter to reduce the residual of the erroneous measurement, the residuals of the *other* measurements will be affected. The converging value of the PE is thus for the value that reduces the sum of the weighted residuals for all of the measurements. This is the reason why the estimation of line susceptance is accurate, since a small change in the estimated value from the true value will affect the estimation of the other measurements in a high degree. In comparison, since the line conductance is so much smaller than the line susceptance, it may be changed significantly more without affecting the residuals of the remaining measurements. Thus, the estimation of both line conductance and shunt susceptance may prove to be highly inaccurate when even small errors in the measurement devices are present.

Furthermore, the estimation of all parameters was found to be more sensitive to errors in the voltage measurements than for the power flow measurements. The explanation for this is that there is no direct system measurement function for the voltage that is depending on the parameters, as is the case for the power flow measurements (according to equations (3.16)-(3.19)). Instead, the estimated parameters affect the power flow measurement functions that in turn affect the estimation of the voltage. This results that the parameters may be tuned significantly before the residuals of the erroneous voltage measurement is decreased and the estimation may thus be inaccurate even for low measurement errors.

To summarize, the PE algorithm is found to be most accurate in estimating the line susceptance, and is in general inaccurate for estimating the line conductance and the shunt susceptance. The measurement devices within the transmission grid are commonly rated for errors of ± 0.5 %, but the accuracy is in general greater than this value and estimation of the line susceptance for suspected erroneous branches is thus accurate in most cases. A method of evaluating the magnitude of the measurement errors prior to the PE should be performed, in order to verify that the PE will be sufficiently accurate. The bad data detection method by using the LNRT that was presented in section 3.3.3 could be a good test to verify that the residuals are not too large to perform a PE. In real life testing, the weighting matrices may be tuned specifically according to the accuracy of the measurements. For example, since the measurement of the reactive power has been found to be relatively sensitive to errors, the weight of this measurement may be chosen to a lower value. This will of course have a direct effect on the outcome and accuracy of the PE.

7.4 Alternative method of line resistance estimation

The accuracy of the alternative method for line resistance estimation was found to be more accurate than by using the ordinary method of PE. The accuracy was in this case found to be significantly less dependent on errors in the voltage measurement. Instead, errors in the power flow measurements were found to be of most significance to the accuracy. The simplifications in the theory in section 4.4 are causing some of the errors in the estimation. If the load flow situation will be altered and a heavy load applied, the assumption that $V_s \approx V_r$ will no longer be true. Hence, the estimation error in this case is both due to measurement error and to model simplification errors.

This estimation method also requires a more experimental approach and one of the drawbacks is that the results are not directly included within the actual SE model. Instead, the estimation will have to take place after the actual SE has already been performed, and then a reiteration of the SE algorithm will have to be performed. In the same way as for the ordinary PE, the alternative method of estimating the resistance should be carried out after a prior estimation of the magnitude of the measurement errors.

A vertically shifted curve also provides information that there is a probable linear error in either one or both of the power flow measurements. An inspection and calibration of the measurement devices could thus be performed if such errors are found. However, the problem remains in establishing in what end of the branch the linear error is located. The resistance estimation could also be improved by taking this information into account. If either one of the power flow measurements are compensated with the same level as the estimated linear error, the estimation of the line resistance could be significantly enhanced, even if the correct measurement value is compensated.

8 Conclusions and future work

The following section summarises the results and the main conclusions of the report in relation to the aims of the thesis.

Parameter and model errors sensitivity:

- Model errors due to not fully transposed transmission lines are found to affect the phase values of transmission lines considerably. However, if the averaged phase values are used for the analysis, it is found that the resulting average values are differing only marginally from the equivalent single-phase model values. Thus, if averaged phase values are used in the analysis the model errors may be assumed to have a reduced impact on the output of the SE.
- Parameter errors affect the output of the SE in various extents and errors in the line susceptance are found to have the largest effect. The level of measurement redundancy will affect the accuracy of the SE, and reduced measurement redundancy will in general increase the estimation errors.
- For the analysis of a network, the current power flow level was found to significantly affect the impact that parameter errors have on the estimation. A low load on one bus and higher load on the remaining buses resulted in the largest relative estimation errors due to parameter errors. Furthermore, undesirable combinations of parameter errors were found to increase the estimation errors significantly. In order to estimate the magnitude of estimation errors caused by parameter errors, each grid configuration and power flow state would have to be examined individually.

Feasibility of using parameter estimation to increase accuracy of state estimation:

- Parameter estimation was found to be very accurate in estimating the line susceptance in most cases, except for higher levels of measurement errors. Line conductance and shunt susceptance were found to be significantly harder to estimate and even very small measurement errors resulted in misleading parameter estimations. By using parameter estimation under conditions of high accuracy, the estimation errors of the SE were found to decrease significantly.

- The alternative method of estimating the resistance/line conductance was found to be more resilient to errors in the measurement infrastructure. However, the estimation was still sensitive to errors in the power flow measurements and the accuracy may in general not be sufficiently accurate.

8.1 Future work

There are several aspects of the impact that parameter and model errors have on the output of the SE that could be further examined. To begin with, there is very limited literature regarding the actual uncertainty of line parameters, both due to varying effects such as weather and uncertainty due to computational errors of the parameter. More research within this area would be required in order to better evaluate both the magnitude and the probability of parameter errors. Furthermore, more research should be assigned into further developing tools for evaluating the effect that parameter errors have on the output of the SE.

The concept of parameter estimation is still somewhat unexplored. More work should be assigned to examine the feasibility of PE in larger networks when linear measurement errors are present. Furthermore, this report has only examined the accuracy of the so called augmented SE algorithm to estimate line parameters. More effort should thus be assigned to examine the accuracy of other proposed PE algorithms.

More research should also be put into examining exactly how the results of the thesis may be used to develop tools for determining errors in the measurement infrastructure. Such a method could potentially save significant amounts of resources due to fewer actual measurement inspections as well as provide better and more reliable parameter data base values. However, more accurate parameter values do not only result in possibilities to detect measurement errors, but may also enhance the overall continuous operation of the power system. The economic benefits of such an improvement may be vast, but in order to actually implement PE as an accepted method, the economic and monetary benefits of an increased accuracy of state estimation should first be evaluated.

9 Bibliography

[1] S. A. Boyer, *SCADA: Supervisory Control and Data Acquisition*, 3rd Edition, Research Triangle Park: ISA - The Instrumentation, Systems, and Automation Society, 2004.

[2] N. R. Shivakumar and J. Amit, “A Review of Power System Dynamic State Estimation Techniques,” in *Power System Technology and IEEE Power India Conference, 2008. POWERCON 2008. Joint International Conference,* pp. 1-6, 12-15 October 2008. DOI: 10.1109/ICPST.2008.4745312

[3] A. S. Debs and G. Contaxis, “Estimation of Model Parameters for Power System Monitoring and Control,” NSF Grant GK-37474, Atlanta, 1976.

[4] P. Zarco and A. G. Expósito, “Power System Parameter Estimation: A Survey,” in *Power Systems, IEEE Trans.,* vol. 15, no. 1, pp. 216-222, Feb. 2000. DOI: 10.1109/59.852124

[5] SWEDAC, *STAFS 2009:8 Swedacs föreskrifter och allmänna råd om mätsystem för mätning av överförd el, 15 February 2015*. [Online]. Available: www.swedac.se/sv/Dokument/STAFS/Swedacs-foreskrifter-och-allmanna-rad-om-matsystem-for-matning-av-overford-el/. [Accessed 23/02 2016]

[6] A. S. Debs, “Estimation of Steady-State Power System Model Parameters,” *Power Apparatus and Systems, IEEE Trans.* vol. PAS-93, no. 5, pp. 1260-1268, Sept. 1974. DOI: 10.1109/TPAS.1974.293849

[7] I. W. Slutsker and K. A. Clements, “Real Time Recursive Parameter Estimation in Energy Management Systems,” in *Power Systems, IEEE Trans.* vol. 11, no. 3, pp. 1393-1399, Aug. 1996. DOI: 10.1109/59.535680

[8] O. Alsac, B. S. Vempati and A. Monticelli, “Generalized State Estimation,” in *Power Systems, IEEE Trans.* vol. 13, no. 3, pp. 1069-1075, May 1998. DOI: 10.1109/PICA.1997.599382

[9] T. V. Cutsem and V. H. Quintana, “Network parameter estimation using online data with application to transformer tap position estimation,” in *IEE Proceedings C - Generation, Transmission and Distribution* , vol. 135, no. 1, pp. 31-40, Jan. 1998. DOI: 10.1049/ip-c.1988.0004

[10] T. A. Stuart and C. J. Herget, “A Sensitivity Analysis of Weighted Least Squares State Estimation for Power Systems,” in *Power Apparatus and Systems, IEEE Trans,* Vols. PAS-92, no. 5, pp. 1696 - 1701, Jan. 1973. DOI: 10.1109/TPAS.1973.293718

[11] A. Abur and A. G. Expósito, *Power System State Estimation*, New York: Marcel Dekker, Inc, 2004.

[12] D. J. Glover, S. S. Mulukutla and T. J. Overbye, P*ower System Analysis and Design*, Stamford: Global Engineering, 2012.

[13] H. Saadat, *Power System Analysis*, New York: McGraw-Hill Companies, 1999.

[14] A. J. Wood and B. F. Wollenberg, *Power Generation Operation and Control*, New York: John Wiley & Sons, Inc, 1996.

[15] Å. Björck, *Numerical Methods for Least Squares Problems*, Linköping: SIAM, 1996.

[16] M. Grewal, *Kalman Filtering:Theory and Practice with MATLAB*, New Jersey: Wiley-IEEE Press, 2015.

[17] Power Transmission System Planning Software PSS®E, ver 33. Siemens, Germany, Munich.

[18] P. M. Anderson, *Analysis of Faulted Power Systems*, New York: Wiley-IEEE Press, 1995.

[19] J. Ofungwu, Statistics in Practice : *Statistical Applications for Environmental Analysis and Risk Assessment*, New Jersey: Wiley, 2014.

Appendix A

The voltage and power flow measurement data that is being used in the simulations is presented here, along with the actual parameter data. The power flow data illustrated in Figure 15 - Figure 17 is measured on a single branch within the Swedish transmission grid during 96 hours. The parameter values for the examined single branch are presented in Table 12. All the data used in the simulation of the 4-bus network are presented in Table 13 and Table 14.

The subscript for both the parameter and power flow values represents the impedance respectively the power flow between the nodes with the same numbers as for the subscript. Thus, the impedance Z_{12} represents the impedance between node 1 and node 2 and so on. For voltages the subscript represents the voltage values of that particular bus.

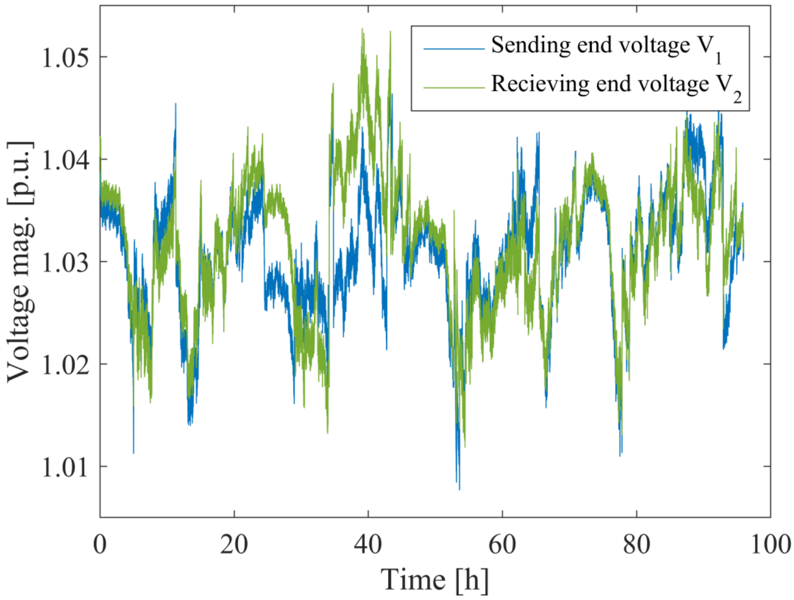

Figure 15. Voltage measurement data from the sending and receiving end of the analysed branch

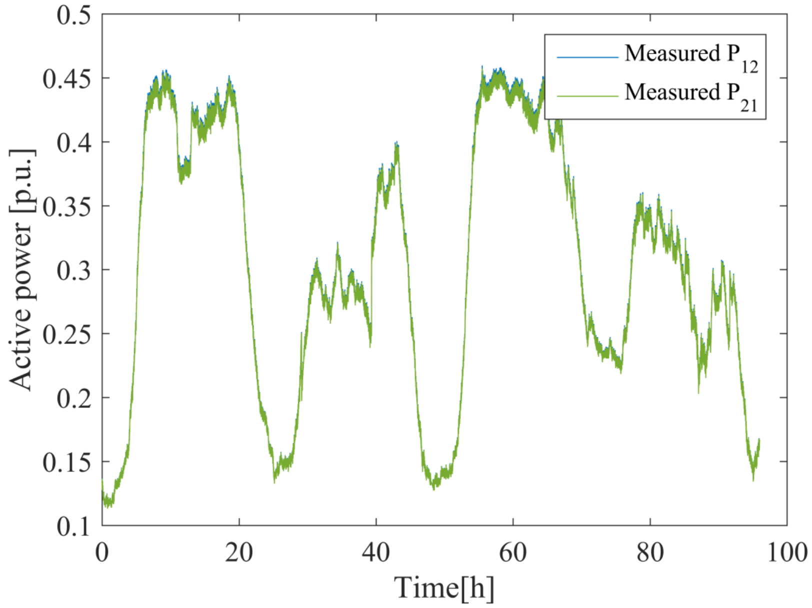

Figure 16. Active power flow measurement in the sending and receiving end

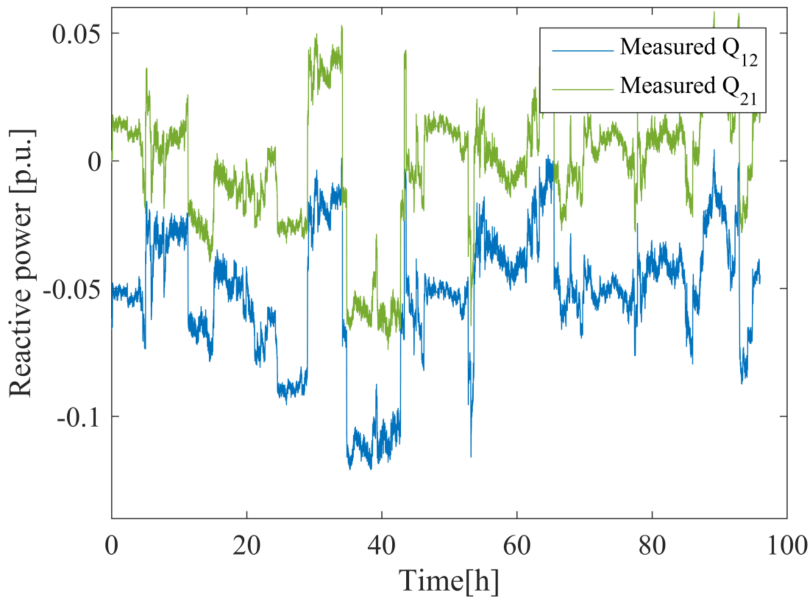

Figure 17. Reactive power flow measurement in the sending and receiving end

Table 12. Parameter values for the examined transmission branch

	Parameter value [p.u.]
Total line conductance (g_{12})	0.0116
Total line susceptance (b_{12})	0.1693
Total shunt susceptance $(bs_1 + bs_2)$	0.06347

Table 13. Branch parameters for the 4-bus network

	Parameter value [p.u.]
Z_{12}	0.097 + j0.92072
Y_{12}	j0.01569/ 2.0
Z_{23}	0.0006 + j0.0041
Y_{23}	j0.00006 / 2.0
Z_{24}	0.0187 + j0.17722
Y_{24}	j0.00302 / 2.0
Z_{45}	0.0 j0.0001
Y_{45}	j0.0 / 2.0
Z_{46}	0.03961 + j0.299508
Y_{46}	j0.005007 / 2.0

Table 14. Perfectly “measured” power flows and voltages for the 4-bus network

	Measured values	
	Case 1	**Case 2**
V_1 **[p.u.]**	1	1
V_3 **[p.u.]**	0.988	1.021
V_5 **[p.u.]**	0.99	1.024
V_6 **[p.u.]**	0.992	1.025
$P_{12} + jQ_{12}$ **[MW+jMVAr]**	209.36 + j2.842	57.429 − j35.461
$P_{32} + jQ_{32}$ **[MW+jMVAr]**	−150 + j5	−30 + j5
$P_{54} + jQ_{54}$ **[MW+jMVAr]**	−35 + j5	−7 + j5
$P_{64} + jQ_{64}$ **[MW+jMVAr]**	−20 + j5	−20 + j5

Appendix B

The full result tables from simulation 5.2.2 are presented in this section. The error is introduced for either a line parameter or for a measurement and the SE algorithm is then performed. The error value is then computed by comparing the estimated values with the true, perfect measurement values.

Table 15. Relative estimation errors for different parameter errors and load flows for a 4-bus network. 20 % of rated power in bus 6 and 100 % of rated power in remaining buses

Error In [%]	g_{12}	b_{12}	bs_1	g_{23}	b_{23}	bs_{23}	g_{24}	b_{24}	bs_{24}	g_{54}	b_{54}	bs_{54}	g_{64}	b_{64}	bs_{64}
V_1	0.094	-0.094	-0.021	0.00	0.000	0.000	0.003	-0.007	0.004	0	0	0	0.001	-0.002	0.009
V_3	-0.042	0.016	-0.001	-0.001	0.000	-0.000	0.006	-0.015	-0.002	0	0	0	0.002	-0.006	0.002
V_5	-0.033	0.039	0.011	0.000	-0.000	-0.000	-0.005	0.012	-0.002	0	0	0	0.002	-0.007	-0.003
V_6	-0.022	0.057	0.019	0.000	0.000	0.000	-0.004	0.011	0.001	0	0	0	-0.005	0.015	-0.005
P_{12}	0.028	-0.220	-0.105	0.000	-0.000	-0.000	0.000	-0.003	-0.022	0	0	0	0.001	-0.002	-0.036
P_{32}	-0.018	0.060	0.029	-0.000	0.000	0.000	0.002	-0.007	0.011	0	0	0	0.001	-0.003	0.020
P_{54}	-0.117	0.264	0.121	-0.001	0.001	0.001	0.005	-0.017	0.040	0	0	0	0.002	-0.008	0.074
P_{64}	-1.437	-3.086	-1.474	-0.002	-0.010	-0.007	-0.052	0.048	-0.367	0	0	0	-0.010	0.012	-0.634
Q_{12}	-20.842	171.791	29.065	-0.027	0.072	0.045	-1.058	3.403	2.005	0	0	0	-0.452	1.343	2.331
Q_{32}	3.053	22.812	8.820	0.020	0.047	0.035	-0.087	0.526	1.774	0	0	0	-0.093	0.315	2.822
Q_{54}	5.123	17.941	7.600	0.002	0.049	0.034	0.214	-0.224	1.810	0	0	0	0.013	0.020	3.148
Q_{64}	5.916	10.954	5.272	-0.012	0.043	0.028	0.416	-0.834	1.522	0	0	0	0.327	-0.770	3.104

Table 16. Relative estimation errors for different parameter errors and load flows for a 4-bus network. 20 % of rated power in bus 6 and 20 % of rated power in remaining buses

Error in [%]	g_{12}	b_{12}	bs_1	g_{23}	b_{23}	bs_{23}	g_{24}	b_{24}	bs_{24}	g_{54}	b_{54}	bs_{54}	g_{64}	b_{64}	bs_{64}
V_1	0.026	-0.138	-0.022	0.000	0.000	0.000	0.001	-0.008	0.004	0	0	0	0.001	-0.002	0.009
V_3	-0.011	0.057	-0.002	0.000	0.000	0.000	0.003	-0.015	-0.002	0	0	0	0.002	-0.006	0.001
V_5	-0.008	0.046	0.010	0.000	0.000	0.000	-0.002	0.012	-0.002	0	0	0	0.002	-0.006	-0.003
V_6	-0.006	0.036	0.019	0.000	0.000	0.000	-0.002	0.010	0.001	0	0	0	-0.005	0.014	-0.006
P_{12}	-0.037	0.252	-0.207	0.000	0.000	-0.001	-0.003	0.020	-0.059	0	0	0	-0.001	0.003	-0.103
P_{32}	0.022	-0.178	0.283	0.000	0.000	0.001	0.004	-0.030	0.074	0	0	0	0.002	-0.007	0.132
P_{54}	0.046	-0.520	1.243	0.000	0.000	0.006	0.009	-0.064	0.299	0	0	0	0.000	-0.012	0.521
P_{64}	-0.353	1.202	-1.425	0.000	0.000	-0.007	-0.028	0.125	-0.378	0	0	0	-0.014	0.026	-0.662
Q_{12}	0.555	-2.925	-1.873	0.000	-0.001	-0.004	0.040	-0.237	-0.184	0	0	0	0.035	-0.103	-0.225
Q_{32}	0.953	-2.310	9.549	0.004	-0.003	0.039	-0.029	0.225	1.957	0	0	0	-0.081	0.281	3.157
Q_{54}	1.470	-4.985	8.391	0.001	0.001	0.038	0.109	-0.505	2.002	0	0	0	0.019	-0.002	3.500
Q_{64}	1.642	-6.291	5.985	-0.002	0.004	0.031	0.201	-1.054	1.694	0	0	0	0.313	-0.757	3.419

Table 17. Estimation errors for different measurement errors with a magnitude of 0.5 %. 20 % of rated power in bus 6 and 20 % of rated power in remaining buses

Err. in [%]	V_1	V_3	V_5	V_6	P_{12}	P_{32}	P_{54}	P_{64}	Q_{12}	Q_{32}	Q_{54}	Q_{64}
V_1	-0.229	0.105	0.080	0.055	0.001	0.000	0.000	0.000	-0.006	-0.000	0.000	0.000
V_3	0.100	-0.363	0.135	0.126	0.000	0.000	0.000	0.000	0.001	0.000	0.000	0.000
V_5	0.075	0.133	-0.357	0.144	0.000	0.000	0.000	0.000	0.002	0.000	0.000	0.000
V_6	0.052	0.125	0.144	-0.327	0.000	0.000	0.000	0.000	0.003	-0.000	0.000	0.000
P_{12}	0.529	-0.120	-0.286	-0.105	-0.129	0.064	0.015	0.042	-0.012	0.004	0.004	0.005
P_{32}	-0.481	-0.141	0.389	0.213	0.245	0.125	-0.029	-0.083	0.021	-0.005	-0.006	-0.006
P_{54}	-1.636	0.076	1.046	0.428	1.055	-0.533	-0.125	-0.354	0.097	-0.021	-0.022	-0.023
P_{64}	2.940	-0.161	-1.737	-0.784	0.324	-0.191	-0.045	-0.132	-0.102	0.026	0.028	0.029
Q_{12}	-4.609	1.198	1.863	2.364	0.000	-0.002	0.000	0.001	-0.279	0.015	0.011	0.008
Q_{32}	-8.272	12.745	2.153	-5.249	0.153	0.021	0.006	0.020	0.754	-0.139	-0.135	-0.127
Q_{54}	-11.877	1.840	10.901	1.073	0.171	0.016	0.006	0.027	0.576	-0.135	-0.145	-0.145
Q_{64}	-12.927	-5.580	-0.059	25.775	0.166	0.004	0.005	0.037	0.335	-0.110	-0.127	-0.157

Table 18. Estimation errors for different measurement errors with a magnitude of 0.5 %. 20 % of rated power in bus 6 and 100 % of rated power in remaining buses

Err. in [%]	V_1	V_3	V_5	V_6	P_{12}	P_{32}	P_{54}	P_{64}	Q_{12}	Q_{32}	Q_{54}	Q_{64}
V_1	-0.229	0.103	0.077	0.051	0.000	-0.000	0.000	0.0001	0.000	-0.000	-0.000	-0.000
V_3	0.104	-0.361	0.136	0.125	-0.001	-0.001	-0.000	0.0001	-0.000	0.000	0.000	-0.000
V_5	0.077	0.135	-0.357	0.144	0.000	0.000	-0.000	0.0001	-0.000	0.000	0.000	0.000
V_6	0.052	0.124	0.144	-0.326	0.002	0.001	0.000	-0.0001	-0.000	-0.000	0.000	0.000
P_{12}	0.081	-0.033	-0.043	0.032	-0.138	0.084	0.019	0.0109	0.001	0.002	0.002	0.002
P_{32}	-0.131	-0.033	0.090	0.066	0.179	-0.1267	-0.029	-0.0167	-0.000	-0.001	-0.001	-0.001
P_{54}	-0.461	-0.009	0.254	0.192	0.769	-0.539	-0.126	-0.0717	-0.000	-0.003	-0.003	-0.004
P_{64}	2.782	-0.019	-1.482	-0.485	0.963	-1.003	-0.242	-0.1414	0.009	0.027	0.028	0.029
Q_{12}	152.563	-13.280	-18.863	-22.104	3.024	0.793	0.181	0.0916	-0.257	-0.159	-0.112	-0.068
Q_{32}	-8.467	11.805	1.364	-5.666	1.656	0.332	0.095	0.0574	-0.053	-0.132	-0.126	-0.117
Q_{54}	-12.120	1.062	9.993	0.587	1.590	0.268	0.089	0.0600	-0.039	-0.128	-0.137	-0.136
Q_{64}	-13.144	-6.127	-0.657	25.055	1.293	0.147	0.064	0.061	-0.021	-0.103	-0.120	-0.151

Appendix C

In the following section the main parts of the MATLAB code used to perform the parameter estimation of line susceptance is presented. The estimation of line conductance and shunt susceptance is performed in a similar manner, but with the state defined for these parameters instead.

Initiate a flat start and define states

```
% Flat start: Voltages = 1 p.u. and angles = 0 degrees:
x1 = 0;    % delta2
x2 = 1;    % V1
x3 = 1;    % V2
x4 = b12m; % Our estimated parameter is defined as a state
x = [x1 x2 x3 x4]';  % State matrix
```

Load all measured values and define the parameter as a measurement

```
% Create a for loop with the length of: length(t) = number of measurements
for k=1:length(t)
z = [FPs(k) FQs(k) abs(FUs(k)) -FPr(k) -FQr(k) FUr(k) b12m]';
% z is the measurment vector

    i=0;
    deltaX=[1 1 1 1]';

    % When the difference between two iterations is lower than this value
    % -> algorithm has converged
    while abs(max(deltaX)) > 0.0000000005
    i=i+1;
```

Define angles and all the system measurement functions

```
% Defining angles
th12 = 0 - x1; %Theta12
th21 = x1;     %Theta21
% Defining system measurement functions for estimated values, f(x):

f1 = x2^2*g12 - x2*x3*(g12*cos(th12)+x4*sin(th12));            % P12
```

```
f2 = -x2^2*(bsh12+x4) - x2*x3*(g12*sin(th12)-x4*cos(th12));     % Q12
f3 = x2;                                                         % V1
f4 = x3^2*g12 - x2*x3*(g12*cos(th21)+x4*sin(th21));              % P21
f5 = -x3^2*(bsh12+x4) - x2*x3*(g12*sin(th21)-x4*cos(th21));     % Q21
f6 = x3;                                                         % V2
f7 = x4;
F = [f1 f2 f3 f4 f5 f6 f7]';
```

Defining the Jacobian of the system measurement functions

```
% Defining the Jacobian of f(X):
h11 = -x2*x3*(g12*sin(th12)-x4*cos(th12));                  %dP12/dTh2
h12 = -x3*(g12*cos(th12)+x4*sin(th12))+2*x2*g12;            %dP12/dV1
h13 = -x3*(g12*cos(th12)+x4*sin(th12));                     %dP12/dV2
h14 = -x2*x3*sin(th12);                                     %dP12/db12

h21 = x2*x3*(g12*cos(th12)+x4*sin(th12));                   %dQ12/dTh2
h22 = -x3*(g12*sin(th12)-x4*cos(th12))-2*x2*(x4+bsh12);     %dQ12/dV1
h23 = -x2*(g12*sin(th12)-x4*cos(th12));                     %dQ12/dV2
h24 = -x2^2 + x2*x3*cos(th12);                              %dQ12/db12

h31 = 0;                                                    %dV1/dTh2
h32 = 1;                                                    %dV1/dV1
h33 = 0;                                                    %dV1/dV2
h34 = 0;                                                    %dV1/db12

h41 = x3*x2*(g12*sin(th21)-x4*cos(th21));                   %dP21/dTh2
h42 = -x3*(g12*cos(th21)+x4*sin(th21));                     %dP21/dV1
h43 = -x3*(g12*cos(th21)+x4*sin(th21))+2*x3*g12;            %dP21/dV2
h44 = -x2*x3*sin(th21);                                     %dP21/db12

h51 = -x2*x3*(g12*cos(th21)+x4*sin(th21));                  %dQ21/dTh2
h52 = -x3*(g12*sin(th21)-x4*cos(th21));                     %dQ21/dV1
h53 = -x2*(g12*sin(th21)-x4*cos(th21))-2*x3*(x4+bsh21);     %dQ21/dV2
h54 = -x3^2+x2*x3*cos(th21);                                %dQ21/db12

h61 = 0;                                                    %dV2/dTh2
h62 = 0;                                                    %dV2/dV1
h63 = 1;                                                    %dV2/dV2
h64 = 0;                                                    %dV2/db12

h71 = 0;                                                    %db12/dTh2
h72 = 0;                                                    %db12/dV1
h73 = 0;                                                    %db12/dV2
h74 = 1;                                                    %db12/db12

Hx = [h11 h12 h13 h14;...
```

```
        h21 h22 h23 h24;...
        h31 h32 h33 h34;...
        h41 h42 h43 h44;...
        h51 h52 h53 h54;...
        h61 h62 h63 h64;...
        h71 h72 h73 h74];
```

Performing SE algorithm to minimize weighted residuals

```
% Performing minimization of estimations and measurements
HxT = Hx';
Gm = HxT*inv(W)*Hx;
deltaX = inv(Gm)*Hx'*inv(W)*(z-F);
x = deltaX + [x1; x2; x3; x4];
x1 = x(1); x2 = x(2); x3 = x(3); x4 =x(4);
```

Calculating new weighting factor for the estimated parameter and updating the initial, "measured" value of the parameter. This algorithm is then performed for each of the measured values and the final value of b12m is the estimated value of the inductance

```
InvG = inv(Gm);
W(end)=InvG(end);
West(k) = W(end);
b12m=b12m-(z(7)-F(7));
```